

UNCLASSIFIED

AD NUMBER
AD889403
NEW LIMITATION CHANGE
TO Approved for public release, distribution unlimited
FROM Distribution authorized to U.S. Gov't. agencies only; Test and Evaluation; 1971. Other requests shall be referred to Air Force Armament Laboratory [DLIF], Eglin Air Force Base, Florida 32542.
AUTHORITY
AFATL ltr, 30 Mar 1976

THIS PAGE IS UNCLASSIFIED

2

AFATL-TR-71-87

AD 889403

AD No. _____
DDC FILE COPY

INCENDIARY POTENTIAL
OF EXOTHERMIC INTERMETALLIC
REACTIONS

LOCKHEED PALO ALTO RESEARCH LABORATORY

TECHNICAL REPORT AFATL-TR-71-87

JULY 1971

DDC
RECEIVED
DEC 2 1971
C

Distribution limited to U. S. Government agencies only; ~~test and evaluation~~
~~test and evaluation~~; distribution limitation applied
July 1971. Other requests for this document must be referred
to the Air Force Armament Laboratory (DLIF), Eglin Air Force
Base, Florida 32542.

AIR FORCE ARMAMENT LABORATORY

AIR FORCE SYSTEMS COMMAND • UNITED STATES AIR FORCE

EGLIN AIR FORCE BASE, FLORIDA

175

ACCESSION for _____
POSTED WHITE SYSTEM ☐
DATE DATE SYSTEM ☒
UNANNOUNCED ☐
CLASSIFICATION _____
BY _____
DISTRIBUTION/AVAILABILITY CODES
DIST. AVAIL. CODE/IF SPECIAL
B

Incendiary Potential Of Exothermic Intermetallic Reactions

Alexander P. Hardt

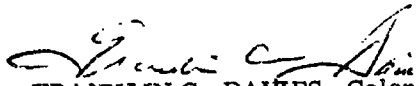
Distribution limited to U. S. Government agencies only; ~~this report~~
~~is not to be distributed outside the~~
~~DLIF~~ *Test and evaluation*; distribution limitation applied July 1971. Other requests
for this document must be referred to the Air Force Armament
Laboratory (DLIF), Eglin Air Force Base, Florida 32542.

FOREWORD

This study was performed by the Lockheed Palo Alto Research Laboratory, Lockheed Missiles & Space Company (LMSC), 3251 Hanover Street, Palo Alto, California 94304, under Contract F08635-70-C-0063 for the Armament Development Test Center (AFATL), Eglin Air Force Base, Florida. The task was monitored by Dr. Robert L. McKenney, Jr. (DLIF), AFATL Program Scientist, and carried out between 19 March 1970 and 19 May 1971.

The research was performed under the direction of Dr. A. P. Hardt, LMSC Program Manager. The writing of the computer codes and the subsequent analytical study was accomplished by Dr. P. V. Phung, Research Scientist. Experimental measurements were performed by Messrs. R. W. Holsinger, J. R. Toolson, and F. J. Smith, LMSC Program Engineers. The suggestions by Dr. J. F. Riley are gratefully acknowledged. The contractor report number is LMSC-D177523.

This technical report has been reviewed and approved.


FRANKLIN C. DAVIES, Colonel, USAF
Chief, Flame, Incendiary and
Explosives Division

ABSTRACT

The objective of this research was to study the incendiary potential of inter-metallic reactions. A thorough literature review of the thermochemistry of exothermic alloy formation, measurement of the reaction rates, reaction temperatures, and ignition characteristics of loose and pressed binary and tertiary mixed powders provided basic information for incendiary assessment. The borides, carbides, and aluminides of titanium, zirconium, and nickel were found to offer the greatest promise. The data were compared with those obtained by a computerized heat transfer analysis of rod shaped and hollow cylindrical geometries. The rate controlling parameters were found to be particle size, thermal conductivity, heat of reaction, and diffusivity. In most cases it was found that reaction characteristics were independent of particle size distribution, particle shapes, contamination, bulk density, and compaction. Experimental data agreed with analytical predictions. Intermetallic reactions were deemed to be a novel class of reactions and the results were found to have wide applicability in improving the performance characteristics of pyrotechnic, ordnance, and incendiary devices.

Distribution limited to U. S. Government agencies only; this report documents the study of the incendiary potential of intermetallic reactions; distribution limitation applied July 1971. Other requests for this document must be referred to the Air Force Armament Laboratory (DLIF), Eglin Air Force Base, Florida 32542.

TABLE OF CONTENTS

Section	Page
I INTRODUCTION	1
II THE THERMOCHEMISTRY OF INTERMETALLIC REACTIONS	2
1. Literature Survey	2
2. Experimental Studies	7
a. Materials and Equipment	7
b. Experimental Results	11
c. Analysis of Reaction Products	13
d. Thermal Transport Properties	17
III STUDY OF REACTION RATES	21
1. Experimental Study	21
2. Experimental Data	21
a. Effect of Particle Size	24
b. Effect of Ambient Temperature	24
c. Effect of Heat of Reaction	24
3. Analytical Study of Reaction Rates	25
a. The Mathematical Model	25
b. Results of Mathematical Analysis	28
IV STUDY OF IGNITION CHARACTERISTICS	32
1. Experimental Study	32
2. Analytical Study of Ignition Characteristics	34
3. Application of Ignition Studies to Incendiaries	39
a. Ignition and Reaction of Thermites and Thermates	39
b. Use of Intermetallic Reactions in Tracer and Incendiary Munitions	43

TABLE OF CONTENTS (CONCLUDED)

Section		Page
	c. Formulation of Intermetallic Reaction Mixtures	43
V	APPLICATION OF INTERMETALLIC REACTION OF PYROTECHNIC AND ORDNANCE TECHNOLOGY	46
	1. Characteristics of Intermetallic Reactions	46
	2. Present Applications of Intermetallic Reactions	47
	3. Future Application of Intermetallic Reactions	47
VI	CONCLUSIONS AND RECOMMENDATIONS	49
Appendix		
I	SOURCES AND SPECIFICATIONS OF REAGENTS	50
II	PROGRAM STATEMENTS FOR LINEAR RATE STUDIES	51
III	PROGRAM STATEMENTS FOR ANALYTICAL IGNITION ENERGY STUDY	58
IV	METHOD FOR COMPUTING IGNITION CHARACTERISTICS	62
	REFERENCES	63

LIST OF FIGURES

Figure	Title	Page
1	Photomicrograph of Typical Starting Mixture, 100 ×	14
2	Photomicrograph of a Partially Completed Intermetallic Reaction, 500 ×	15
3	Photomicrograph of Incomplete Intermetallic Reaction, 5000 ×	16
4	Intermetallic Reaction Product - Starting Mixture at Room Temperature, 500 ×	18
5	Intermetallic Reaction Product, Starting Mixture Preheated, 3000 ×	19
6	Mold for Burning Rate Specimens	22
7	Temperature-Time History of a Reaction Between Amorphous Boron and -200 + 325 Mesh Titanium	24
8	Computed Reaction Characteristics of Titanium-Carbon Reaction Mixture	27
9	Ignition History of -325 Mesh Titanium-Boron Mixture	33
10	Computed Ignition Times of Intermetallic Reaction Mixtures	35
11	Computed Ignition Fluences of Intermetallic Reaction Mixtures	36
12	Illustration of Mathematical Approach to the Determination of Minimum Ignition Energy	38
13	Ignition Energies of Intermetallic Reaction Mixtures	40
14	Assembled Incendiary Demonstration Unit	41
15	Titanium-Boron Reaction Mass With Intermetallic Reaction Igniter	42
16	Computer Run of Hypothetical Intermetallic Mixture, Ignited by Transient Heat Source	44

LIST OF TABLES

Table	Title	Page
I	Intermetallic Reactions of the Alkali Metals	3
II	Intermetallic Reactions of the Alkaline Earths	4
III	Intermetallic Reactions of Group III Elements: Borides	5
IV	Intermetallic Reactions of Group III Elements: Aluminides	6
V	Intermetallic Reactions of Group III Elements: Rare Earths and Actinides	7
VI	Intermetallic Reactions of Group IV Elements: Carbides	8
VII	Intermetallic Reactions of Group IV Elements: Silicides	9
VIII	Intermetallic Reactions: Miscellaneous Systems	10
IX	Tabulation of Experimental Data	12
X	Thermal Transport Properties of Intermetallic Reaction Mixtures	20
XI	Experimental Linear Reaction Rates	23
XII	Computed Reaction Characteristics	29
XIII	Effect of Diffusivity Prefix on Reaction Rate	30
XIV	Effect of Activation Energy of Reaction Rate	30
XV	Computed Ignition Characteristics	37
Appendix		
IV-1	Method of Ignition Flux Calculation	62

LIST OF SYMBOLS

A	component A
B	component B
C_p	heat capacity (cal/g°K)
D	diffusivity (cm ² /sec)
D_t	thermal diffusivity, $\kappa/C_p\rho$, (cm ² /sec)
D_o	diffusivity prefix (cm ² /sec)
E	energy of activation for diffusion (cal/mole)
ϵ	emissivity
F_i	ignition fluence, (cal/cm ²)
\dot{F}_i	ignition flux (cal/cm ² -sec)
$H_T - H_{ST}$	enthalpy of a substance at temperature T relative to its standard state at 298°K (cal/mole)
H_R	heat of reaction (cal/mole)
κ	thermal conductivity (cal/cm-sec-°K)
P	pressure (atm)
Ψ	particle size, diffusion barrier thickness (cm)
ψ	diffusion barrier thickness (cm)
Q	heat of reaction (cal/cm ³)
Q_i	ignition energy (cal/g)
r	radius of incendiary body (cm)
R	gas constant (cal/mole-°K)
ρ	density (g/cm ³)
σ	Stefan-Boltzmann constant (cal/cm ² -sec-°K ⁴)
T	temperature (°K)
T_o	temperature of heatsink (°K)
T_i	ignition temperature (°K)
t	time (sec)
v	linear reaction rate (cm/sec)
x	increment along incendiary body or incremental increase of radius (cm)

SECTION I

INTRODUCTION

Pyrotechnic reactions are of two kinds: (1) gas phase reactions which are controlled by pressure and surface area, such as black powder and single or double base propellants; and (2) condensed phase reactions which are controlled by thermal and molecular transport, such as thermite and intermetallic reactions.

Exothermic intermetallic reactions are of practical importance because of their high heat of reaction and the magnitude of the resulting temperature. Intermetallic reactions occur with the release of a heat of solution as the result of the reaction of finely powdered metals. If the heat released in reacting or forming an alloy is sufficient, the reaction will provide an intense source of thermal radiation. The resulting temperature may be sufficient to melt or even vaporize some constituents which can then react with oxygen, releasing additional heat. Intermetallic reactions which provide intense sources of thermal radiation and high temperatures have potential applications in advanced incendiaries and pyrotechnics.

One purpose of this study was to review the thermochemistry of exothermic intermetallic reactions and to present a discussion of such condensed phase processes. In keeping with the generally accepted scope of intermetallic reactions, boron, carbon, and silicon have been considered to be metallic while phosphorus, sulfur, arsenic, and selenium have been excluded.

Other objectives of this research were to measure the heats of reaction, the reaction temperatures, reaction rates, and ignition characteristics for promising candidates; to determine the effects of composition, particle size, compaction, and reaction mechanism on the incendiary potential; to compare these data with those obtained on thermate; and to provide a scientific and engineering basis for explaining the findings.

The term "incendiary potential" refers to thermochemical and kinetic characteristics and does not include the assessment of the effects of these reactions on a target. As a result of this study, intermetallic reactions were found to provide a novel means of improving the reliability and reaction characteristics of existing thermate-based incendiaries and, furthermore, to alter ignition delays and ignition energy requirements of other types of pyrotechnic devices such as smoke cartridges, signal markers, delay fuzes, and tracer munitions.

SECTION II

THE THERMOCHEMISTRY OF INTERMETALLIC REACTIONS

1. LITERATURE SURVEY

A thorough review of the thermochemistry of exothermic intermetallic reactions was undertaken to assure complete coverage of all promising binary combinations of elementary constituents. The search focused on two areas: equilibrium thermodynamic data on the heats of formation (heats of reaction), and applications of exothermic intermetallic reactions to problems of a metallurgical or pyrotechnic nature.

Thermodynamic data are plentiful. Unfortunately, little agreement exists and rarely do the authors define their reference conditions with care. The laborious task of critical evaluation of the published data has been performed during the last two decades by R. Hultgren and his associates at the University of California (1, 2).

As a result of the study presented here, it was found that favorable thermodynamics is a necessary but not a sufficient condition to insure a self-sustained reaction. Special experimental and analytical studies were performed to define the additionally required conditions.

In the survey, a few applications of exothermic intermetallic reactions were found such as a commercial Al-Pd composite (3) called "Pyrofuze" and a reported similar application of magnesium-platinum and lead-lithium (4). More recent applications are discussed in Section V of this report.

Tables I through VIII list the exothermic heats of reaction of binary mixtures of various elements of the first through the fourth groups of the periodic table with elements of the third through the eighth groups. The compounds listed under the heading "System" indicate the stoichiometric proportion of the reagents as well as the end product to which the thermal data have reference. It must be understood that the reacting system consists of mixtures of the finely powdered elements, and the conclusions drawn in this study have validity regardless of whether the actual phase described by the stoichiometric formula is formed.

Heats of formation are reported on a molar basis for the compound as written. They are equal to the heats of reaction where the starting materials are elements in their standard state. The literature source cited refers to this enthalpy value. Assuming that a system consists of a stoichiometric blend of the powders compressed to the bulk density of the parent elements, it is possible to compute the energy density as well. The density of the intermetallic product is usually significantly greater than the density of the unreacted mixture. Because the theoretical bulk density is rarely achieved, intermetallic reactions can be expected to generate a product with an appreciable void fraction.

TABLE I. INTERMETALLIC REACTIONS OF THE ALKALI METALS

Group	System	Heat of Reaction			Adiabatic Reaction Temperature (°C)*	Lowest Melting Point (°C)	Ref.
		kcal/mole	cal/g	cal/cm ³			
III	LiAl	-15.1	-443	-555	860 (l)	109	5
IV	LiSn	-16.8	-134	-575	1000 (l)	109	1
	LiPb	-14.6	-68	-465	960 (l)	109	1
	NaSn	-10.2	-71.4	-254	800 (s)	98	1
	Na ₂ C ₂	-9.6	-137	-161	460 (s)	98	6
V	LiSb	-21.8	-170	-700	1060 (l)	109	1
	LiBi	-18.4	-85.5	-535	1000 (l)	109	1
	NaSb	-15.8	-109	-375	780 (l)	98	1
	KBi	-18.0	-55	-204	980 (l)	64	1

* Based on an ambient temperature of 298°K.

The adiabatic reaction temperature T_R is that temperature at which the enthalpy of formation, ΔH_f , equals the enthalpy of the product, namely

$$(\Delta H_f)_{T_R} = (H_T - H_{ST})_{T_R}$$

Where the enthalpies of the intermetallic product are not known, the enthalpies of the starting materials were used (1,2):

$$(\Delta H_f)_{T_R} = (H_T - H_{ST})_{A, T_R} + (H_T - H_{ST})_{B, T_R}$$

The state of the product at the adiabatic reaction temperature was checked against the phase diagram and the appropriate symbol (s, s-l, l, and l-v) was used to denote solid, liquid, and vapor states. The adiabatic temperature is the maximum temperature which the reaction can achieve. It is the upper boundary condition imposed upon a computer code calculation of intermetallic reactions as well as a guide in predicting whether a self-sustained intermetallic reaction is possible.

The initial step in the reaction process is thought to be solid-solid diffusion between the reagent particles. The resulting heat of reaction will not be conducted away from the reaction zone if the thermal conductivity of the mixture is low.

TABLE II. INTERMETALLIC REACTIONS OF THE ALKALINE EARTHS

Group	System	Heats of Reaction			Adiabatic Reaction Temperature (°C)(*)	Lowest Melting Point (°C)	Ref.
		kcal/mole	cal/g	cal/cm ³			
I	LiMg	-2.56				109	1
	CuMg	-5.0				650	2
II	CaMg ₂	-9.4	-106	-175	540 (s)	650	2
III	Al ₂ Ca	-52.5	-560	-1150	1440 (l-v)	650	1
	Y Mg	-31.0	-274	-912	1670 (l)	650	7
	CeMg	-18.3	-111	-523	920 (l)	650	7
	UMg	-41.4	-157	-1570	1940 (l)	650	7
	UBe ₁₃	-39.3	-111	-520	500 (s)	1132	8,2
	PuBe ₁₃	-35.7	-100	-476	450 (s)	640	2
	ThMg ₂	-15.2	-54	-317	700 (s)	650	9
IV	SnMg ₂	-18.9	-113	-450	890 (s)	890	1
	SnCa ₂	-75.0	-379	-1110	1484 (l-v)	232	1
	SnBa ₂	-90.0	-240	-1000	2125 (l-v)	232	1
	PbCa ₂	-50.7	-172	-705	1440 (l-v)	327	1
	PbBa ₂	-69	-143	-715	1640 (l-v)	327	1
V	NbBe ₅	-46.4	-336	-1300	1390 (s)	1277	10
	Sb ₂ Ba ₃	-87.5	-133	-563	1560 (l)	630	1
	Bi ₂ Ba ₃	-72.5	-87.3	-169	1400 (l)	271	1

(*) Based on an ambient temperature of 298°K.

Because of the small size of the individual grains, the resulting temperature rise may therefore be sufficient to cause the reactant or the product to melt so as to destroy the diffusion barrier and expose fresh reagent. If no melting occurs, the diffusion barrier may reduce the reaction rate to the point of quenching. The most important factors which promote quenching are:

TABLE III. INTERMETALLIC REACTIONS OF GROUP III ELEMENTS: BORIDES

Group	System	Heats of Reaction			Adiabatic Reaction Temperature (°C)(*)	Lowest Melting Point (°C)	Ref.
		kcal/mole	cal/g	cal/cm ³			
II	MgB ₆	-22.4	-251	-600	645 (s)	650	11
III	Y B ₆	-24	-156	-503	700 (s)	1509	12, 13
	LaB ₆	-114	560	-2410	2230 (l-s)	1509	12, 13
IV	CB ₄	-17	-326	-758	750 (s)	2030	14
	SiB ₃	-7	-76.4	-177	230 (s)	1410	15
	TiB ₂	-71.6	-1155	-4040	3770 (l)	1668	2
	ZrB ₂	-78.0	-690	-3330	3400 (l)	1852	2
	HfB ₂	-78.6	-394	-3450	3380 (s-l)	2030	2
V	VB	-32.6	-528	-2500	2400 (s)	1900	16
	NbB ₂	-58.6	-511	-2870	2900 (s)	2030	17
	TaB ₂	-43.9	-216	-2610	2400 (s)	2030	17
VI	CrB ₂	-30	-408	-1880	1500 (s)	1875	13
	MoB ₂	-23	-196	-1280	1260 (s)	2030	13
	W ₂ B ₅	~-35	~-83	-1350	960 (s)	2030	13
VII	MnB ₂	-19	-248	-1140	800 (s)	1245	13

(*)Based on an ambient temperature of 298°K.

- (1) High thermal conductivity
- (2) Large particle size
- (3) Adiabatic reaction temperature too low to promote adequate diffusion

Hence, it is concluded that where the adiabatic reaction temperature does not exceed the melting point of the product, the reactions are not self-sustaining. This condition is shown by the notation(s) behind the adiabatic reaction temperature. Examples are CaMg₂, UBe₁₃, ThMg₂, NbBe₅, MgB₆, YB₆, CrB₂, MoB₂, W₂B₅, MnB₂, CuAl, CrAl₃, MnAl, SmB₆, CaC₂, B₄C, VC, NbGe₂, NbC, TaC, Cr₇C₃, Mo₂C, WC, Mn₇C₃, Mg₂Si, Cr₅Si₃, MnSi₂, FeSi, CoSi, NiSi, WSi₂, and CuPd. Many of the

TABLE IV. INTERMETALLIC REACTIONS OF GROUP III ELEMENTS: ALUMINIDES

Group	System	Heats of Reaction			Adiabatic Reaction Temperature (°C)(*)	Lowest Melting Point (°C)	Ref.
		kcal/mole	cal/g	cal/cm ³			
I	CuAl	-9.8	-108	-756	870 (s)	660	18
	LiAl	-15.1	-443	-555	860 (l)	109	5
II	CaAl ₂	-52.5	-560	-1150	1440 (l-v)	650	1, 18
III	B ₂ Al	-36	-740	-1850	1900 (s)	660	19
	LaAl ₄	-41.2	-166	-780	1222 (s-l)	660	1
IV	TiAl ₂	-28.8	-314	-1100	1370 (l-s)	660	2
	ZrAl ₂	-40.8	-281	-1200	1650 (l-s)	660	20
V	VAl ₃	-26.0	-198	-792	750 (s)	660	18
VI	CrAl ₃	-16	-120	-430	520 (s)	660	1, 18
VII	MnAl	-10.2	-124	-586	530 (s)	660	1, 18
VIII	FeAl	-12.14	-147	-725	1150 (s)	660	1, 19
	CoAl	-26.4	-308	-1600	1580 (s)	660	1
	NiAl	-28.1	-329	-1710	1639 (s-l)	660	2
	PdAl	-43.7	-327	-2890	2380 (l)	660	3
	PtAl	-48	-216	-2510	2800 (l)	660	2
(*)Based on an Ambient Temperature of 298°K.							

other systems are marginal in that low heat output would make a purely incendiary application questionable or high thermal conductivities would cause quenching.³ Systems with the maximum potential (energy density in excess of 2000 cal/cm³ and reaction temperature in excess of 2000°C) include LaB₆, TiB₂, ZrB₂, PdAl, PtAl, BeC₂, TiC, ZrC, VSi₂, and NbSi₂. Because of high cost and short supply, one should exclude systems requiring La, Pd, and Pt. The systems selected on this basis permit a study over a wide range of compositions, particle size, and ambient temperature and resulted in several new concepts for pyrotechnic or incendiary applications.

TABLE V. INTERMETALLIC REACTIONS OF GROUP III ELEMENTS: RARE EARTHS AND ACTINIDES

Group	System	Heats of Reaction			Adiabatic Reaction Temperature (°C)(*)	Lowest Melting Point (°C)	Ref.
		kcal/mole	cal/g	cal/cm ³			
Rare Earths	SmB ₆	-50	-232	-1050	960 (s)	1072	22
	CeB ₆	-84	-410	-1850	1700 (s)	795	12
	CeAl ₄	-31.2	-126	-458	900 (s)	660	1
	PrAl ₄	-54.0	-216	-800	1430 (s-l)	660	1
Actinides	ThB ₄	-52.0	-189	-1360	1550 (s)	1750	12
	UB ₄	-60	-214	-1950	1770 (s)	1132	12
	UAl ₄	-29.8	-86	-565	760 (s)	660	23
	PuAl ₄	-43.2	-123	-820	1130 (s)	660	24

(*)Based on an ambient temperature of 298 °K.

2. EXPERIMENTAL STUDIES

a. Materials and Equipment

Starting materials were procured from commercial sources and used without any further attempt at purification or sieving. Appendix I lists the suppliers and the nominal specification of these powders. The powders were further characterized by scanning electron microscopy which permitted a determination of geometry, size, and size distribution through measurements of the resulting photographs. Appendix I also lists the most typical or rate determining particle size. It is this value which will be used in the subsequent discussion of the data.

Some powders are sensitive to air and are shipped under oil or water; these were dried in a vacuum chamber and manipulated in an argon-filled glove box.

Determinations of the reaction temperatures and emissivities were performed using fast response pyrometry. For events of brief duration, the calibrated anode current of a photomultiplier tube was used to measure brightness-temperature. The response time of this signal was a fraction of a millisecond, and the signal was monitored using a fast oscilloscope or a recording oscillograph. Two instruments

TABLE VI. INTERMETALLIC REACTIONS OF GROUP IV ELEMENTS: CARBIDES

Group	System	Heats of Reaction			Adiabatic Reaction Temperature (°C)(*)	Lowest Melting Point (°C)	Ref.
		kcal/mole	cal/g	cal/cm ³			
I	Na ₂ C ₂	-9.660	138	196	410 (s)	98	6
II	BeC ₂	-57.7	-1750	-3720	2770 (l-v)	1277	13
	CaC ₂	-15.0	-222	-388	900 (s)	838	6
	SrC ₂	-20.2	-182	-460	1300 (s)	768	25
	BaC ₂	-19.5	-121	-391	1200 (s)	714	25
III	B ₄ C	-17	-326	-758	750 (s)	2030	14
	Al ₄ C ₃	-53.4	-371	-965	1400 (s)	660	26
	LaC ₂	-29	-178	-870	1700 (s)	920	27
	CeC ₂	-27.9	-170	-880	1560 (s)	795	28
	UC ₂	-25	-95.5	-1082	1300 (s)	1132	29
	ThC ₂	-46	-179	-1280	2800 (s)	1750	29
IV	SiC	-15.8	-394	-910	1680 (s)	1410	30
	TiC	-44.1	-737	-3270	3600 (l)	1668	2
	ZrC	-47.0	-461	-2460	3800 (l)	1852	2
	HfC	-52.3	-268	-2730	4200 (s)	2222	2
V	VC	-25.9	-412	-1870	2030 (s)	1900	2
	NbC	-33.6	-321	-2060	2730 (s)	2415	2
	TaC	-35.5	-184	-2380	2800 (s)	2896	2
VI	Cr ₇ C ₃	-54.50	-136	-818	780 (s)	1875	2
	Mo ₂ C	-11.01	-57	-482	600 (s)	2610	2
	WC	-9.06	-49	-645	900 (s)	3410	2
VII	Mn ₇ C ₃	-20.2	-48	-300	300 (s)	1245	2
(*)Based on an ambient temperature of 298°K.							

TABLE VII. INTERMETALLIC REACTIONS OF GROUP IV ELEMENTS: SILICIDES

Group	System	Heats of Reaction			Adiabatic Reaction Temperature (°C)(*)	Lowest Melting Point °C	Ref.
		kcal/mole	cal/g	cal/cm ³			
II	Mg ₂ Si	-10.2	-180	-346	540 (s)	650	31
	CaSi	-36	-528	-950	1670 (l)	838	13
III	Y Si	-32.2	-275	-1000	1835 (s-l)	1410	13
	CeSi ₂	-50.0	-255	-1100	1810 (l)	795	13
	ThSi ₂	-42.0	-146	-963	1590 (s)	1410	13
	USi ₂	-31.0	-106	-940	1390 (s)	1132	32
IV	CSi	-15.8	-394	-910	1680 (s)	1410	30
	TiSi ₂	-32.1	-308	-924	1610 (s)	1410	2
	ZrSi ₂	-38.1	-259	-1020	1780 (l)	1410	2
V	V Si ₂	-75	-700	-2350	3280 (v-l)	1410	13
	NbSi ₂	-71.6	-480	-2040	3300 (l)	1410	13
	TaSi ₂	-27.8	-117	-806	1570 (s)	1410	2
VI	Cr ₅ Si ₃	-77.6	-227	-1110	1230 (s)	1410	13
	MoSi ₇	-31.3	-206	-940	1550 (s)	1410	2
	WSi ₂	-22.4	-93.4	-670	1230 (s)	1410	13
VII	MnSi _{1.7}	-23.2	-226	-847	1160 (s-l)	1245	33
VIII	FeSi	-19.2	-229	-1000	1410 (s-l)	1410	13
	CoSi	-24.0	-276	-1285	1460 (s-l)	1410	13
	NiSi	-20.5	-236	-110	990 (s-l)	1410	13, 19
(*) Based on an am temperature of 298°K.							

were used: The Br EP-1, and the Infr against a Bureau of against the melting

gineering Company's Photo-Electronic Pyrometer, Model stries Thermodot Model TD-11S. Calibration was ds lamp. Temperatures above 2200°C were checked f refractory metals.

TABLE VIII. INTERMETALLIC REACTIONS: MISCELLANEOUS SYSTEMS

Group	System	Heats of Reaction			Adiabatic Reaction Temperature (°C)(*)	Lowest Melting Point (°C)	Ref.
		kcal/mole	cal/g	cal/cm ³			
I	NaSb	-16.2	-112	-384	892 (l-v)	98	34
	CuPd	-7.57	-44.5	-472	600 (s)	1083	2
II	My ₂ Ge	-25.1	-207	-605	1115 (s-l)	650	35
	Mg ₃ Sb ₂	-38.25	-121	-484	1160 (s)	630	2
	Mg ₂ Sn	-10.1	-62	-145	500 (s)	232	36
III	CeZn	-21.2	-78	-535	1140 (l)	420	37, 38
	PuCd ₁₁	-45.9	-31	-293	570 (s)	321	37
	PuZn ₁₂	-73.3	-71.3	-600	700 (s)	420	37
	U ₂ Zn ₁₇	-95.4	-60	-530	700 (s)	420	39
IV	PdSn	-25.24	-112	-1000	1326 (s-l)	232	40
	Ce ₂ Pb	-39.64	-81.5	-665	1380 (s-l)	327	2
	NbGe ₂	-29.8	-84.4	-524	1170 (s)	937	41
	ZrZn ₂	-37.63	-170	-1165	1450 (l, s)	692	2
V	NbNi	-10.8	71	610	810 (s)	1726	2
(*) Based on an ambient temperature of 298°K.							

Assuming a greybody behavior, the true temperature was measured using a Millietron Two Color Pyrometer. The response time of this instrument was more than 300 msec, and it was only of limited value in the measurement of fast events. Furthermore, the assumption of a greybody was found to be satisfactory only in the study of carbide reactions.

For comparative studies of incendiary effects and for measuring heat flux, radiometers were found to be more powerful tools than pyrometers. For determining temperature profiles as a measure of rate in fast reactions and a measure of the effect of mixture characteristics on ignition characteristics, fast response pyrometers remain the preferred tool.

Heats of reaction were determined as a function of composition in air and/or argon in a Parr bomb calorimeter operating at 1 atm. After blending and pressing, the starting materials were characterized with respect to uniformity and void formations by sectioning and metallographic examination. Following reaction, the degree of reaction was similarly characterized.

Ignition temperatures were measured by the insertion of a fine thermocouple into the pressed reaction body. Mixtures were initiated by wrapping a nichrome wire around the pressed specimen and heating the system electrically. It will be shown in this report that ignition temperatures are affected partly by heat flux and partly by mixture characteristics such as particle size and thermal conductivity.

Other experimental techniques relating to the measurement of reaction rates and ignition rates will be discussed in Sections III and IV of this report.

Measurements of thermal transport properties were of importance in analyzing observed reaction phenomena, and these were made part of this research program. The thermal conductivities were determined from published specific heats and measured thermal diffusivities and densities. Thermal diffusivities were measured using the flash technique (Ref. 21) in which a short duration (< 1 msec) flash from a xenon lamp is deposited on the face of a thin layer or wafer of intermetallic mixture, and the time required for the back face temperature to reach 50 percent of its maximum value is measured oscillographically. This value is used in an analytical expression for the flow of heat through an infinite slab. Corrections for heat losses are applied.

A nominal compaction pressure of 20,000 psi was used throughout this study although it was found that intermetallic reactions are not limited by the compaction pressure, and that most mixtures tend to expand to varying degrees when released from the die.

The performance of intermetallic reactions was compared against that of thermate, TH-3, obtained for this purpose from Eglin Air Force Base.

b. Experimental Results

Table IX presents a summary of the experimental data obtained in this research program. The measurements do not, in all cases, agree with published data. This is probably due to:

- Unreliable published data, particularly where these are derived from solution calorimetric or electrochemical data
- Incomplete reaction because of surface cooling or the presence of local inhomogeneities
- Incomplete reaction because of dead sintering
- Low total enthalpy changes lead to low precision in calorimetry
- Deviations from greybody behavior

TABLE IX. TABULATION OF EXPERIMENTAL DATA

System	Experimental Heat of Reaction (cal/g)		Measured Density	Measured Emissivity	Ignition Temp. in °C Air	Average Reaction Temp. °C	Reference Table No. (This Report)
	Air	Argon					
LiAl	2013	1130	1.30		170	2340	I
LiB	3870	1145	1.23	0.179	200	2500	No publ. data
BeC ₂	No Rx	No Rx			~1200°		VI
TiB	1010	865	2.90	0.444		3010	
TiB ₂	1226	1225	2.45	0.727	550	3000	III
ZrB	647	511	3.08		530	2340	
ZrB ₂	796	799	3.20			3410	III
TaB ₂	355	308	6.81	0.72	410	2315	III
NbB ₂			4.07	0.458		2160	III
TiAl ₂	520	296	3.13		400	1200	IV
ZrAl ₂	400	412	3.20		100	1350	IV
TaAl	150	No Rx	8.60		640	1500	No publ. data
NiAl	440	242	4.74	0.376	640	1700	IV
CeAl ₂			4.1			1100	
TiC	860	813	2.50		600	2050	VI
ZrC	575	412	4.37		550	1540	VI
TaC			5.95		650	1250	VI
TaSi ₂	242	No Rx	5.00		450	1625	VII
NiSi	313	242	3.45	0.168	250	1430	VII
NiB ₂	No Rx	No Rx	3.42				No publ. data
Ni ₂ B					540	930	No publ. data
Ce ₂ Sn		No Rx					(47)
LiMgPb	233	131	6.28		200	1090	No publ. data
Li ₁₀ Pb	435	357	4.0			1820	I
Li ₄ Pb	320	378	4.2		200	1195	I
CeZn ₂	419	118	4.8		50	2300	VIII
Ce ₂ Pb	400	133	6.2		50	1260	VIII
CeMg	642	100	4.5		50	1270	II
Thermate TH-3	1241	1247	3.37	0.275	600	2940	(a)

(a) Computed.

The corresponding published data may be found in the earlier tables of this section by reference to the table number given in the right-hand column of Table IX.

The observed reaction temperatures were in reasonable agreement with the adiabatic reaction temperatures. Where the measured values were higher, it was due to the ignition technique which involved heating the entire sample to the ignition temperature so that the reaction energy was augmented by the ignition energy. In some instances, the reaction energy was increased by reaction with air.

Based on the thermal measurements of this study, summarized in Table IX, it was concluded that the following systems have the greatest incendiary potential:

- Boron with titanium, lithium, or zirconium
- Carbon with titanium or zirconium
- Aluminum with nickel or with mixtures of the above

This appraisal, based on the thermal data only, is in general agreement with the findings of the literature survey.

In addition to these binary systems, the effect of a third component was experimentally investigated. Admixture of a third component, such as aluminum to a boron-titanium mixture, results in heats of reaction between those of Al-B and Ti-B. Other effects on the incendiary potential are due to changes in thermal conductivity, melting point of an intermediate phase, and similar reaction kinetic parameters. These effects are discussed in further detail later in this report. It was shown that ease of ignition and reliability of reaction were improved by lowering the thermal conductivity. This was demonstrated by the addition of small amounts of boron or lamp black to reaction mixtures of relatively high thermal conductivity, such as Ni-Al or thermite. The low mechanical strength of some formulations may be overcome, in part, by the admixture of a binder, such as 1 percent gum arabic, without noticeable effect on performance characteristics.

c. Analysis of Reaction Products

Insight into the reaction mechanism was obtained by pyrometry and by analysis of the intermetallic systems both before and after reaction. Figure 1 shows a section through a pellet of Ti-2B which is quite representative of all the compressed reaction mixtures. The mass appears to be without obvious voids, the titanium (the discontinuous phase) appears to be uniformly distributed, and the particles appear to be elongated or flat and preferentially oriented (normal to the direction of the compression).

The appearance of the reaction product reveals whether the reaction went to completion and whether the reaction occurred in the gas phase or in the liquid phase. Figure 2 shows particles of titanium in a carbon matrix which are surrounded by crusts of the reaction product. This layer of product effectively prevents further reactions. A similar picture (Figure 3) shows particles of tantalum surrounded by

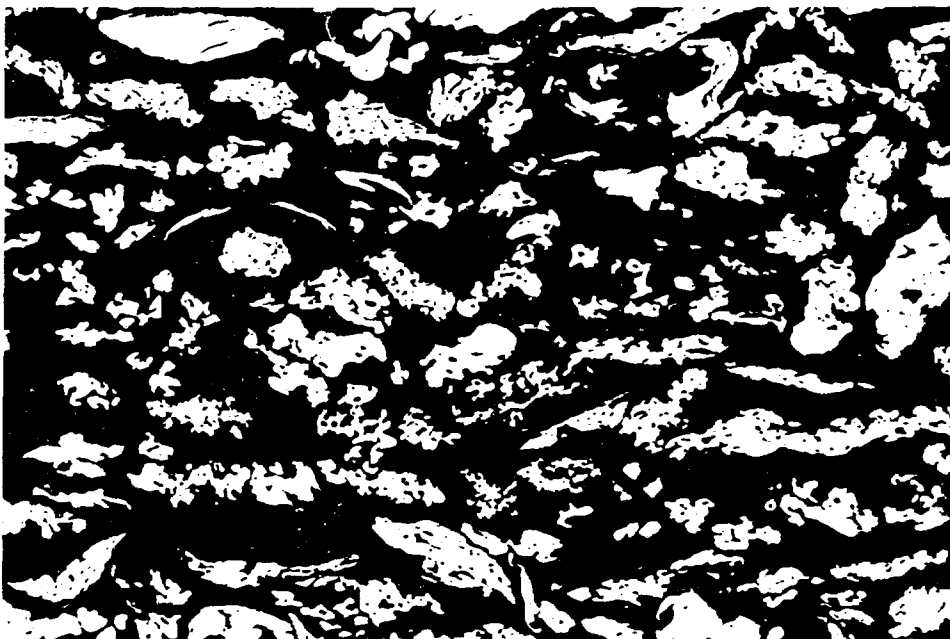


Figure 1. Photomicrograph of Typical Starting Mixture. 100 ×
Titanium powder, 30 μ effective particle size, in continuous matrix of boron powder, 2 μ particle size, pressed at 20,000 psi.

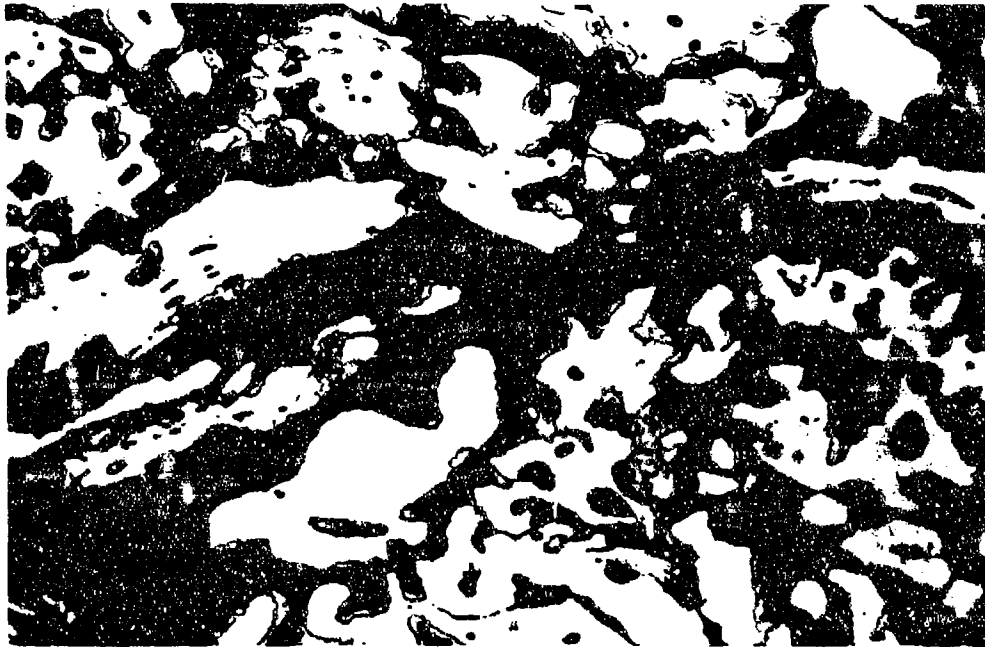


Figure 2. Photomicrograph of a Partially Completed Intermetallic Reaction,
500 x

Titanium powder particles, 30- μ effective particle size in a 0.5- μ graphite matrix, pressed at 20,000 psi, heated to about 800°C for 5 minutes. Metallographic section shows the reaction inhibited by a crust of reaction product which surrounds the metal powder. Such behavior is common when the particle size or the thermal conductance is too large. Such mixtures will sinter but not react in a self-sustained manner.

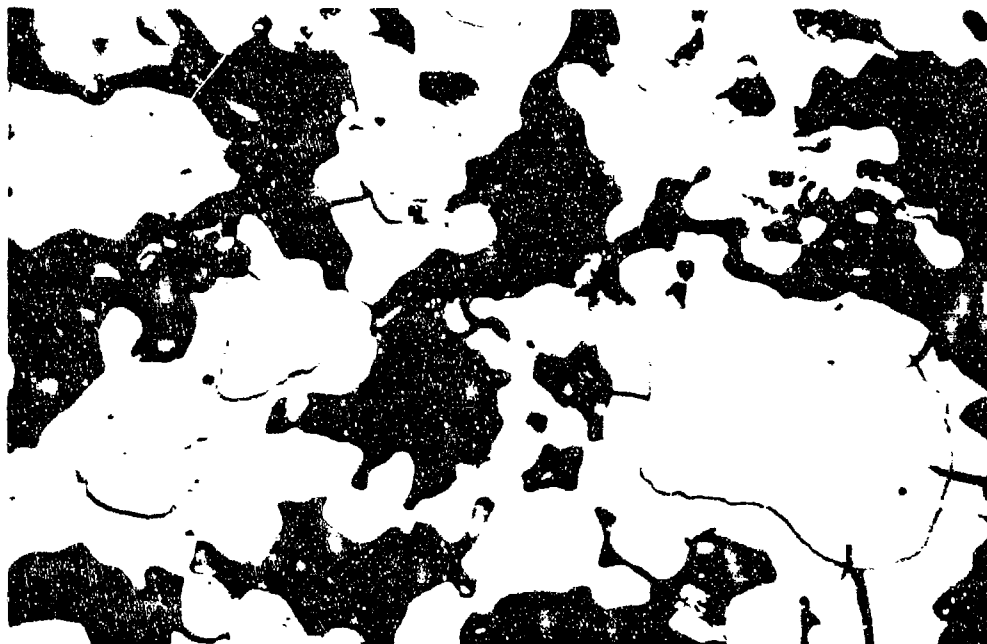


Figure 3. Photomicrograph of Incomplete Intermetallic Reaction, 5000 \times

Tantalum powder, 4- μ effective particle size in 2- μ silicon powder, pressed at 20,000 psi and heated to about 800°C for 5 minutes. Metallographic section shows partial completion of the reaction by formation of successive layers of the various silicide phases. This type of reaction is typical when the reaction temperature is insufficient to melt the reaction product. Such mixtures usually cannot be made to react in a self-sustained manner. At times, preheating of the reaction mixture is effective provided that the self-quenching shown in Figure 2 can be avoided.

several phases of a silicide and immersed in a matrix of silicon. Such systems do not react in a self-sustained manner. Usually it is necessary to reduce the particle size (as for titanium carbide) or increase the ambient temperature so as to raise the reaction temperature above the melting point of the product (as with the tantalum silicide) before the reaction becomes self-propagating. Figure 4 shows the titanium diboride reaction product that is formed when the compressed, unreacted mixture undergoes essentially no preheating prior to ignition. The reaction temperature never approaches the predicted adiabatic reaction temperature but is sufficient (2500-3000°C) to cause melting and crystallization of the product from the liquid phase. The appearance of voids and of a fairly uniform reaction are typical. When a mixture is preheated above ambient temperature, the preheat temperature increases the adiabatic reaction temperature causing the system to react above the boiling point of some of the constituents. Such a phenomenon is accompanied by deposition of crystalline product from the gas phase as shown in Figure 5.

d. Thermal Transport Properties

Table X lists the thermal transport properties of the reaction mixtures selected for this study. The heat capacities are those of the starting materials at ambient temperature. The densities are experimental values and reflect the apparent density of the compressed samples. The experimental method is designed to measure the thermal diffusivity which should, in principle, be independent of density. Table X shows, however, that thermal diffusivities of compressed and uncompressed samples differ by as much as 300 percent, indicating that conductance in fine powders is a complex phenomenon. It appears that, when particles are finely divided, surface effects predominate and the properties of the bulk material can no longer be used. There are no good theoretical approaches for estimating thermal conductivities of fine powders. For this reason, thermal transport data were obtained experimentally for intermetallic mixtures and for the unmixed, but powdered, reactants. These data can be a valuable guide in estimating conductivities of mixtures having compositions which are not listed by serving as aids in interpolation.

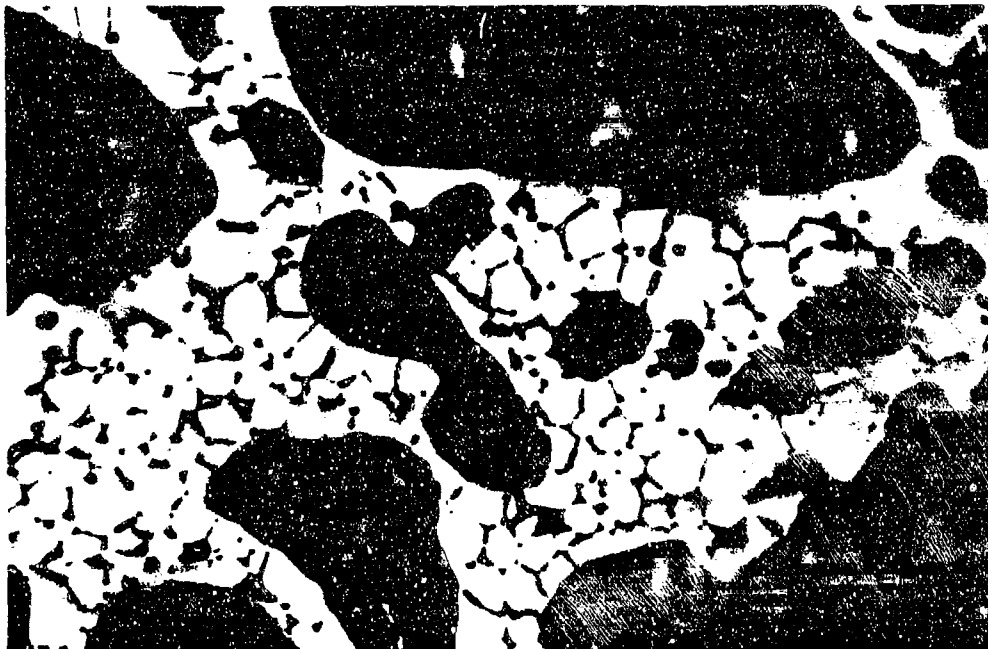


Figure 4. Intermetallic Reaction Product – Starting Mixture at Room Temperature 500 ×

Photomicrograph of TiB_2 reaction product. The material exhibits voids with incipient crystal formation. This is the typical appearance of a product which reacted at a temperature sufficiently high to cause melting but not to produce a vapor phase. This stoichiometric mixture, pressed to 20,000 psi, was ignited with a first fire and within a few milliseconds heated itself to about 2800°C .

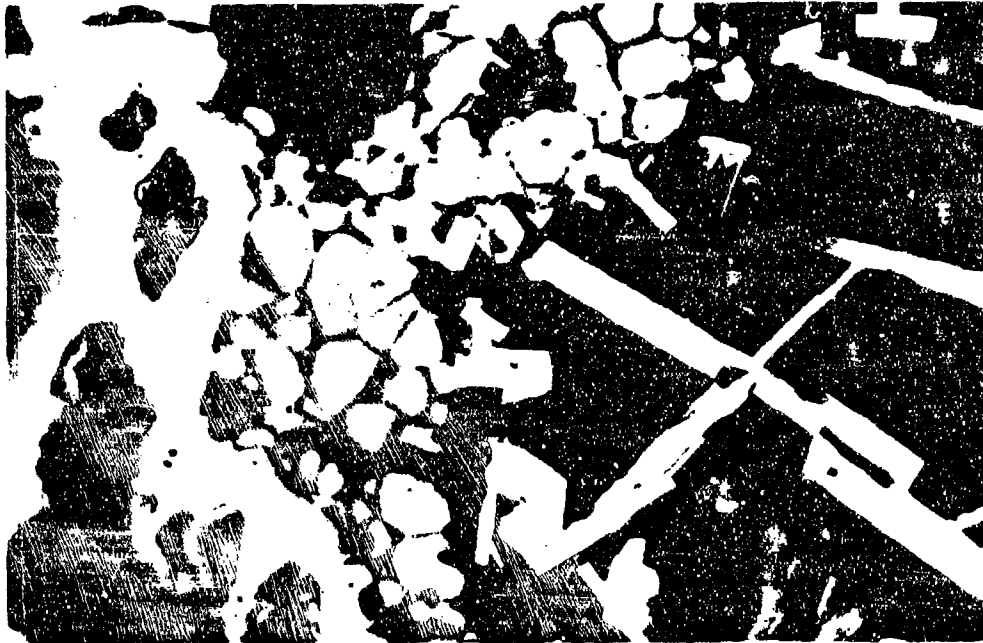


Figure 5. Intermetallic Reaction Product, Starting Mixture Preheated, 3000 ×
Photomicrograph of a TiC reaction product. The material exhibits voids, crystals which appear formed from the liquid phase, and large needle-like crystals which are believed to have been grown from the vapor phase. This is the typical appearance of a product which reacted at a temperature sufficiently high to cause partial vaporization. This stoichiometric mixture of titanium powder in lampblack, pressed at 20,000 psi, was preheated to about 800°C when it suddenly heated itself to a temperature of about 3000°C which was retained for about 2 sec.

TABLE X. THERMAL TRANSPORT PROPERTIES OF INTERMETALLIC REACTION MIXTURES

System	Effective Particle Size	Heat Capacity (cal/g°K)	Density (g/cm ³)	Thermal Diffusivity (cm ² /sec)	Thermal Conductivity (cal/cm sec °K)
Ti-2B					
Uncompacted	60 μ Ti 2 μ B	0.162	0.975	7.6×10^{-4}	1.2×10^{-4}
Uncompacted	10 μ Ti 2 μ B	0.162	0.925	7.19×10^{-4}	1.07×10^{-4}
Pressed	60 μ Ti 2 μ B	0.162	2.32	1.87×10^{-3}	0.7×10^{-3}
Ti-C					
Uncompacted	10 μ Ti 0.5 μ C	0.134	0.571	9.31×10^{-4}	0.64×10^{-4}
Pressed	10 μ Ti 0.5 μ C	0.134	3.28	3.85×10^{-2}	1.73×10^{-2}
Ti-B	10 μ Ti 2 μ B	0.146	2.76	3.81×10^{-3}	1.68×10^{-3}
Ti-3B	10 μ Ti 2 μ B	0.173	2.10	2.76×10^{-3}	1.22×10^{-3}
Zr-2B	20 μ Zr 2 μ B	0.100	2.96	1.68×10^{-3}	5.61×10^{-4}
Zr-C	20 μ Zr 0.5 μ C	0.078	3.65	0.0127	0.00352
Ni-Al	40 μ Ni 30 μ Al	0.141	5.11	0.220	0.156
with 5% B	as above	0.145	4.50	0.081	0.053
with 10% B	as above	0.150	3.95	0.0134	0.008
with 25% B	as above	0.168	2.82	0.0028	0.0013
(Ti-2B with 10% Al)	60 μ Ti 2 μ B 30 μ Al	0.167	2.44	0.00345	0.0014
with 30% Al	as above	0.177	2.45	0.0043	0.0019
with 50% Al	as above	0.188	2.42	0.0085	0.0039
Ti	10 μ 60 μ	0.125	3.63 3.78	0.00935 0.00967	0.00423 0.00447
B	2 μ	0.244	1.31	0.00090	0.00029
Zr	3 μ	0.066	4.35	0.00374	0.00107
Carbon (2/3 graph 1/3 Acet. Black)	0.5 μ	0.17	1.16	0.0115	0.00226
Al	30 μ	0.215	2.66	0.451	0.258
Ni	40 μ	0.105	6.80	0.0526	0.0376
Thermate, TH-3	—	~0.2	2.48	0.0117	0.0058
Thermite	—	0.18	2.75	0.0261	0.0129

All percentages in weight percent. For suppliers of metal powder see Appendix I.

SECTION III

STUDY OF REACTION RATES

1. EXPERIMENTAL STUDY

Two types of reaction rates can be defined: (1) the linear reaction rate, cm/sec, and (2) the mass reaction rate, g/sec-g. In this study, only the linear reaction rate will be considered as it is of greater importance in pyrotechnic and incendiary applications. The linear reaction rate was measured on bars pressed from powder mixtures, as shown in Figure 6. The bar which measured $1/4 \times 1/4 \times 2-1/2$ in., was ignited at one end with a first fire.¹ The rate of migration of the reaction front was followed using either a high-speed motion picture camera (Fastax, 1000 f/sec) or burn wires which were placed on the bar. Both methods gave equivalent results. The motion pictures showed that the reaction front was typically straight and normal to the length of the bar. No flame migration along the surface of the bar was observed as is the case with solid propellant strands; hence, no inhibition of the sides was necessary. The reactions proceeded smoothly, producing a solid rod which remained luminous for up to a minute. The reactions, while in theory not accompanied by a gas phase, usually generated a cloud of particulate matter which was probably a result of adsorbed gases, the vaporization of impurities (oxides, magnesium) from the boron, or the oxidation of the small fraction of the reagents vaporized in the reaction zone. This smoke was sufficient to give erroneous emissivity readings, particularly for the boron reactions.

The high reaction rate of intermetallic reactions, as illustrated in Figure 7, was obtained from the output signal of a fast pyrometer and recorded with an oscilloscope. The compressed mixture was ignited by an electrically heated nichrome wire which, by being wrapped around the sample, assured a fairly uniform temperature distribution throughout the sample at the time of ignition. The temperature rose to the peak within 100msec during which time the reaction was effectively completed. The residual reaction could not have been significant, judging from the steep temperature drop which followed. The reaction time can be prolonged by admixture of coarser particles but at the expense of peak temperature.

2. EXPERIMENTAL DATA

Table XI lists experimental linear reaction rates for various types of intermetallic reactions. Data on Pyrofuze and thermate were included for comparison. The greatest number of parameters were investigated on Ti-2B; therefore, generalized conclusions are well substantiated for this system.

¹It is shown in Section IV of this report that no first fires are necessary for the initiation of intermetallic reactions. For convenience, however, the above study utilized a B/BaCrO₄ mixture.

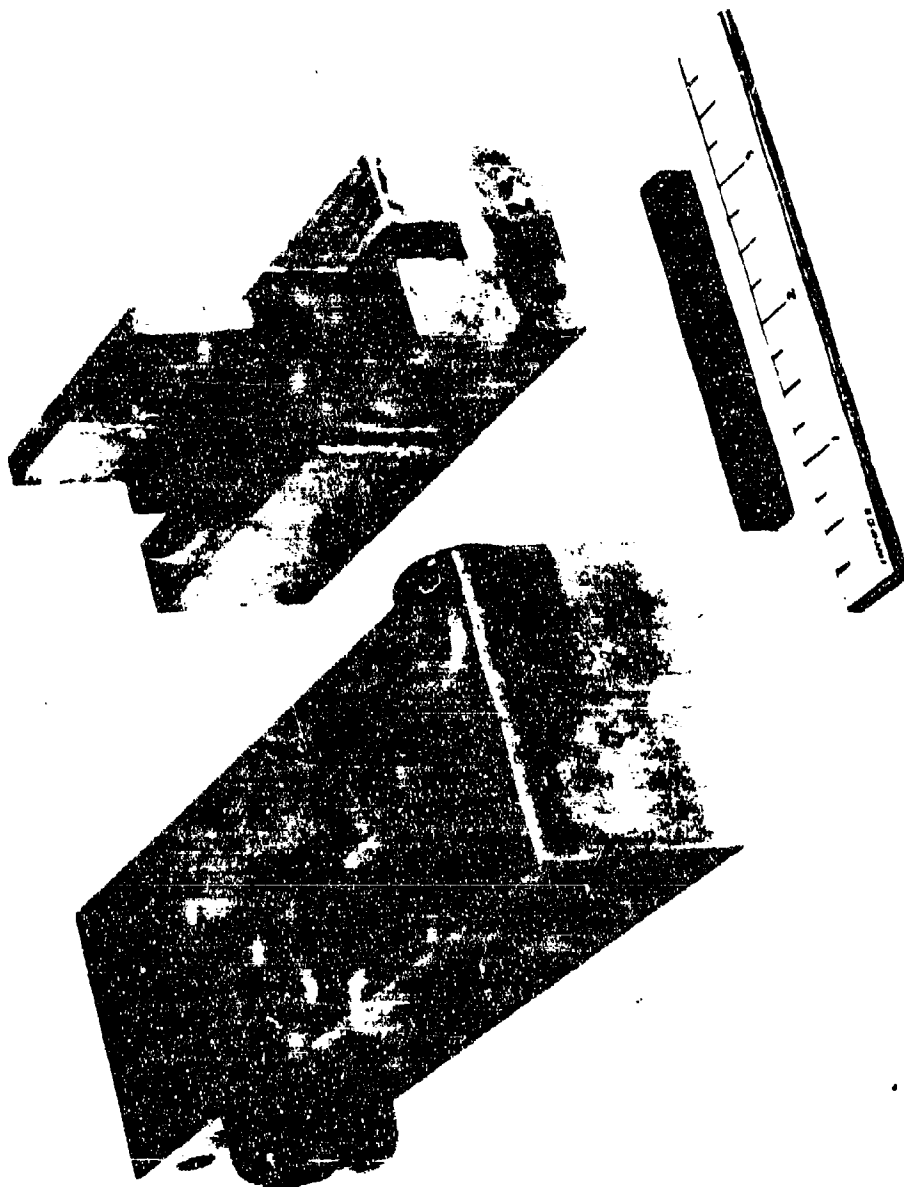


Figure 6. Mold for Burning Rate Specimens.
Sample of pressed reaction mixture is
shown in foreground.

TABLE XI. EXPERIMENTAL LINEAR REACTION RATES

System	Effective Particle Size	Heat of Reaction (cal/g)	Av. Heat Capacity (cal/g-°K)	Density (g/cm ³)	Ambient Temperature (°K)	Thermal Conductivity (cal/cm-sec-°K)	Linear Reaction Rate (cm/sec)
Ti-2B	1 μ Ti	1155	0.306	2.32	300	0.0007	9.44
	2 μ B						
	10 μ Ti	1155	0.306	2.32	300	0.0007	8.33
	2 μ B						
	30 μ Ti	1155	0.306	2.32	300	0.0007	6.57
	2 μ B				200	0.0007	5.67
	60 μ Ti	1155	0.306	2.32	300	0.0007	4.38
	2 μ B						
	60 μ Ti	1155	0.306	2.32	300	0.0007	1.57
	10 μ B						
Ti-2B with 20% reacted TiB ₂	10 μ Ti 2 μ B 10 μ TiB ₂	925	0.306		300		3.59
as above with 40% TiB ₂	as above	695	0.306		300		0.55
Ti-C	1 μ Ti	737	0.226	3.38	300	0.0173	1.83
	0.5 μ C						
	10 μ Ti	737	0.226	3.38	300	0.0173	1.49
	0.5 μ C						
Ti-C with 20% reacted TiC	10 μ Ti 0.5 μ C 40 μ TiC	590	0.226		300		1.04
as above with 40% TiC	as above	442	0.226		300		0.30
Zr-2B	3 μ Zr	690	0.171	2.95	300	0.000561	0.89
	2 μ B						
	10 μ Zr	690	0.171		300		0.15
	2 μ B						
Zr-C	1 μ Zr	461	0.180	3.65	300	0.00352	1.86
	0.5 μ C						
	10 μ Zr						1.02
	0.5 μ C						
Ti-B	60 μ Ti 2 μ B	865	0.27	2.76	300	0.00168	3.88
Ti-3B	60 μ Ti 2 μ B	1137	0.34	2.10	300	0.00122	3.08
Ti-2B with 30% Al	60 μ Ti 2 μ B	690	0.282	2.45	300	0.0043	2.59
	30 μ Al						
as above with 50% Al	as above	533	0.282	2.42	300	0.0085	0.62
Ni-Al	40 μ Ni 30 μ Al	329	0.18	5.11	300 500	0.156	no reaction 3.50
	as above with 5% B	273	0.198	4.50	300	0.054	1.73
	with 10% B	230	0.217	3.95	300	0.0082	0.72
	with 25% B	100	0.273	2.82	300	0.0014	no reaction
Pyrofuze	NA	327	0.17	9	300	0.3	20 (48)
Thermate TH-3	NA	827	~0.20	2.48	300	0.0117	0.275

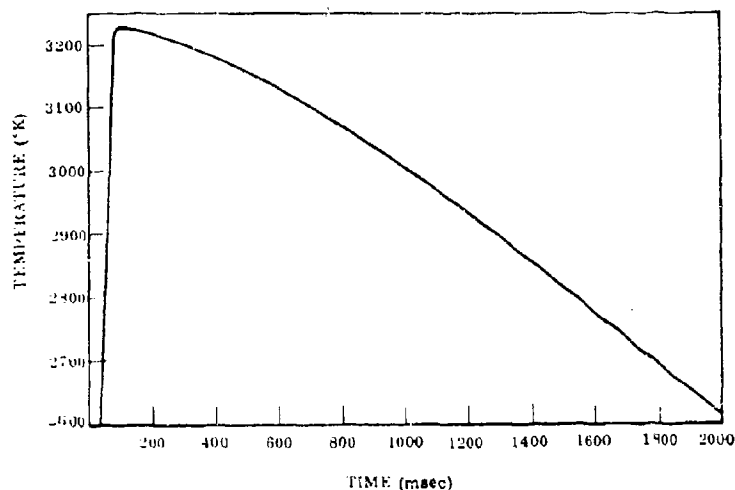


Figure 7. Temperature-Time History of a Reaction Between Amorphous Boron and -200 + 325 Mesh Titanium

a. Effect of Particle Size

Linear reaction rates, shown as the average of several runs, decreased from 9.44 to 4.38 cm/sec linearly when fine boron was used and when the effective particle size of titanium was increased from 1 to 60 μ . When the boron particles were coarse, approaching those of titanium, the reaction rate was further reduced from 4.38 to 1.57 cm/sec.

b. Effect of Ambient Temperature

The effects of preheating and precooling the reaction mixture are shown for Ni-Al and Ti-2B, respectively. The reasons for this behavior are discussed in detail in a subsequent description of analytically obtained results. It shall suffice to say that the ambient temperature affects both the ignition energy and the reaction temperature by causing variations in the diffusivity of the reactants.

c. Effect of Heat of Reaction

Other systems have reaction rates lower than Ti-2B. To resolve whether this difference is due to an inherent property of the reactants or due to the lower reactivity caused by a lower adiabatic reaction temperature, some tests were made with the reactants diluted with various amounts of spent reaction mixture. The effect of this diluent was to reduce the heat of reaction of the mixture without changing other properties

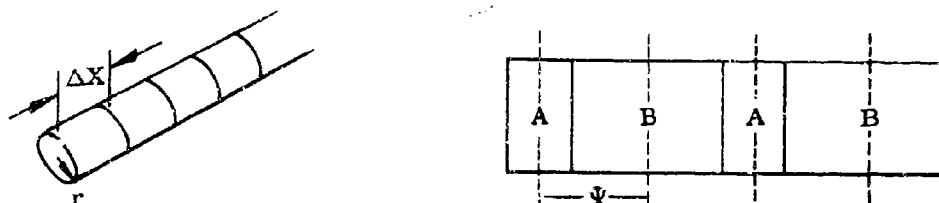
such as heat capacity, diffusion parameters, and thermal conductivity. Linear reaction rates decreased from 8.33 to 0.55 cm/sec as the heat of reaction was decreased from 1155 to 695 cal/g. A similar effect was demonstrated on Ti-C. It was postulated, therefore, that a similar decrease of reaction rate would be observed if very large particles of reactant were added, as these would act as diluent in the reaction zone by soaking up a large amount of sensible heat before undergoing reaction.

Similarly, adding 30 percent aluminum to the mixture decreased the reaction rate from 4.38 to 2.59 cm/sec, chiefly because of the adverse effect on heat of reaction. The reason that the change was not as striking as in the above case involving a diluent is that aluminum increases the thermal conductivity. This effect of thermal conductivity is also visible by comparing the rates of Zr-2B with those of Ti-2B containing 40 percent TiB₂. Both systems have the same heat of reaction, but Ti-2B has a higher reaction rate, partially because of its higher thermal conductivity. The effect of particle size, heat of reaction, and thermal transport will now be considered analytically.

3. ANALYTICAL STUDY OF REACTION RATES

a. The Mathematical Model

The absence of a gas phase greatly facilitates an analytical study of intermetallic reactions. The problem reduces to one of a simple heat transfer analysis uncomplicated by mass transfer considerations or movement of boundaries. Consider a rod of a reactive powder mixture which is heated at one end by an isothermal heat source until the temperature has risen sufficiently to raise the diffusion limited reaction rate to a self-sustaining value. The problem is one of determining the time to achieve ignition temperature (ignition time) and the rate of reaction zone migration along the rod (linear reaction rate).



To accomplish this end, assume that the mixture is composed of particles A and B of effective size Ψ , thermal conductivity κ , heat of reaction Q , and a molecular diffusivity given by

$$D = D_0 \exp \frac{-E}{RT} \quad (1)$$

In each slice Δx the rate of heat generation is related to the diffusivity through Fick's Law:

$$\frac{dQ_1}{dt} = Q \frac{dC}{dt} = QD \frac{d^2 C}{d\psi^2} \quad (2)$$

where ψ is the thickness of the diffusion barrier which increases from 0 to Ψ and dC is the fraction of the reagent, reacting in time interval dt . The heat loss from each section Δx is given by

$$\frac{dQ_2}{dt} = \kappa \frac{d^2 T}{dx^2} + \frac{\epsilon \sigma 2\pi r \Delta x}{\pi r^2 \Delta x} (T^4 - T_o^4) \quad (3)$$

Convective heat loss is ignored in this model. The difference between the heat generation and heat loss in each section corresponds to heat accumulation which is reflected in a rise of temperature. A computer program was written which determines this temperature as a function of time and number of length increments. A listing of statements is given in Appendix II. The input variables are, in part, the particle size, thermal and molecular diffusivity, heat of reaction, ambient temperature, and heat capacity.

Figure 8 shows a sample of computed temperature profiles for a computer experiment utilizing data from the titanium-carbon system. Several features of the experimentally observed phenomena are reflected in these computed data, lending confidence to the belief that the actual reaction mechanism is fairly accurately described. High reaction temperatures and the initiation of the reaction by heat source at 800°K, were observed. This source temperature is far below the melting point of either constituent; thus, the assumption of a solid-solid diffusion limited process appears reasonable. As intermetallic reactions are equally well initiated in vacuum or in an inert atmosphere, the intermediate action of air or of absorbed reactants could not play a significant part. Initiation occurred in less than 25 msec, thereby again describing an experimentally observed phenomenon. The computed reaction rate was high compared with the experimental value, probably because of the fact that the effective diffusivity was overestimated. Several reasons for this are given in the next section. The computed reaction temperature approaches the adiabatic value. Deviation of the computed reaction temperature, 3350°K, from the experimentally observed value, 2320°K, probably is the result of a deviation from an idealized state by the experimental system.

From the described computer output, the following data can be obtained:

- Ignition Time. For each source temperature and each exposure time, the computer output gives the time at which the reaction reaches a self-sustaining level.
- Ignition Energy. The heat transferred during the ignition time into the first slice is the ignition energy. A sample calculation is shown in Appendix IV.
- Ignition Delay. The time required to raise the reaction from the ignition temperature to the steady state reaction temperature.
- Steady State Reaction Temperature. The steady state reaction temperature differs from the adiabatic reaction temperature by the fact that some heat, however small, is lost from the reaction zone to the environment.

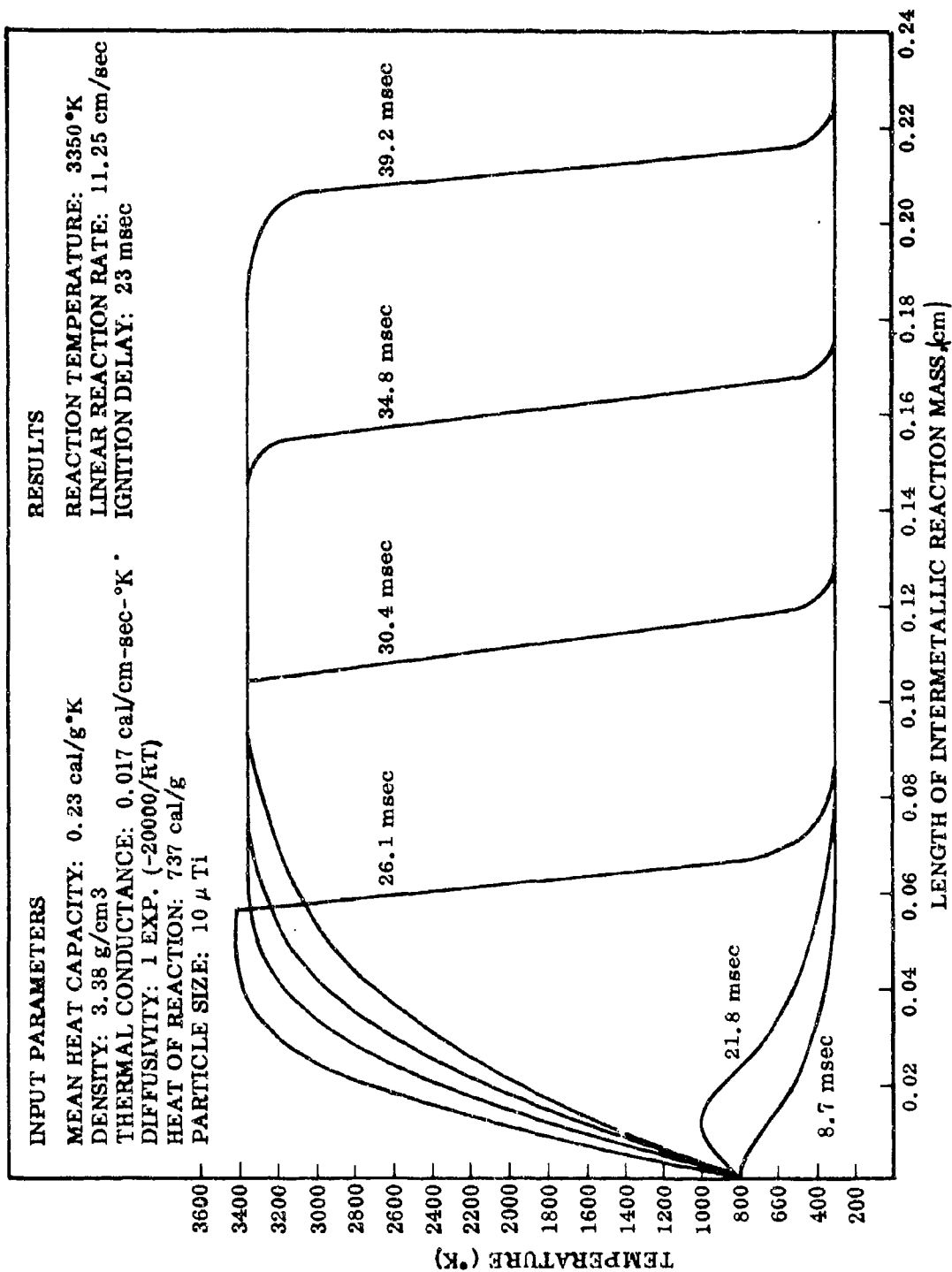


Figure 8. Computed Reaction Characteristics of Titanium-Carbon Reaction Mixture

- Linear Reaction Rate. From the difference in distance between temperature profiles and the corresponding time increments, a velocity of reaction front migration (the linear reaction rate) can be computed.
- Reaction Time. By dividing the thickness of the reaction mass by the linear reaction rate, the reaction time can be obtained.

b. Results of Mathematical Analysis

The computer program was designed for parametric studies of reaction characteristics and so serve as a guide to the most promising experimental studies. The capability of the program to portray actual system behavior depends on how closely the program simulates the reaction mechanism. Such a test of the computerized reaction model by use of experimentally determined properties is shown in Table XII. For this study, the diffusion parameters, prefix, and activation energy were empirically adjustable parameters. Also shown are typical published data for these parameters as obtained by a layer analysis of borodized and carborized metallic specimens (43,44). Some published studies ignore the concentration dependence of diffusivity and shifting of phase boundaries caused by density changes, thereby resulting in well known lack of reproducibility in solid phase diffusivity data. It is felt that not too much reliance should be placed on published diffusivities, except as guides in parametric analysis, because intermetallic reactions proceed by formation of voids and of products having higher densities than the reactants. Systems of such complexity cannot be rigorously treated mathematically.

In comparing the data given in Table XII, it is found that computed reaction rates are higher than experimentally determined rates except for the Ti-2B system. In this system the experimental values are higher. One reason for this, no doubt, is the improper choice of diffusivity values. The discrepancies may also result from changes of reaction mechanism with temperature and changes in conductance due to the formation of voids. The effect of the diffusivity prefix on the rate of a hypothetical intermetallic reaction is given in Table XIII.

A parametric study of the above hypothetical system provided the data in Table XIV on the effect of activation energy on reaction rate.

The computer correctly predicted self-quenching of reactions in systems having high thermal conductivity. Also, the trend expected by the addition of third components or of diluents was predicted correctly. For instance, while third components may increase thermal conductance and thereby increase the reaction rate, this effect may be offset by the lowering of the heat of reaction which causes lower diffusivity and possible quenching. A good example is seen in the addition of aluminum to Ti-2B.

This analytical approach is also useful for obtaining insight into the complex interaction of many parameters. For instance, the quenching of the Ni-Al reaction was overcome when the ambient temperature was raised so as to cause melting of the reaction product and, similarly, lowering of the ambient temperature in Ti-2B mixtures increased the ignition delay until so much heat had soaked into the reaction mixture that the apparent reaction rate was increased. Similar heat transfer analyses of other pyrotechnic reactions should be equally instructive.

TABLE XII. COMPUTED REACTION CHARACTERISTICS

System	Input Parameters		Ignition Time (msec)	Reaction Temperature (°K)	Linear Reaction Rate (cm/sec)		Remarks
	Particle Size (μ)	Diffusion Prefix (cm ² /sec)			Computed	Measured	
Ni-Al	30	1	370		no ignition	no ignition	Actv. En. 56600 cal/mole (43) Amb. Temp. 500°K
	30	0.0047			no ignition	no ignition	
	30	1	77	2250	11.5	3.5	
	30	1	740	1600	3.06	1.73	
	30	10	320	1250	no ignition	1.72	
Ti-2B	2.52	0.5	37		1.61		3.59 cm/sec with 20% diluent Amb. Temp. 200°K
	30	1			no ignition	no ignition	
	60	10	74	3800	0.765	4.38	
	30	10	19	3900	1.46	6.57	
	10	10	2	4000	4.40	8.33	
Ti-C	10	1	14.5	3350	11.25	1.49	Marginal Ignition, required 10 sec. contact with source 1.04 cm/sec with 20% diluent Actv. En. 17000 cal/mole (Ref. 44)
	10	10	2.7	3900	4.27	5.67	
	1	10	0.21	4100	12.70	9.44	
	60	1	5500	1300	0.11	2.59	
	60	1		1300	0.18	0.62	
Zr-2B	3	1	5.75	4100	2.63		1.04 cm/sec with 20% diluent Actv. En. 17000 cal/mole (Ref. 44)
	3	0.01	95	4100	0.51	0.89	
	6	1	11	4100	2.04		
Zr-C	3	1	7.65	2500	2.13	1.86	(Ref. 44)
	3	0.018		2500	0.06		

Except where noted, the activation energy was assumed to be 20,000 cal/mole.
Input Parameters Not Listed are Given in Table XI.

TABLE XIII. EFFECT OF DIFFUSIVITY PREFIX ON REACTION RATE

Diffusivity Prefix (cm ² /sec)	Ignition Time (msec)	Ignition Delay (msec)	Linear Reaction Rate (cm/sec)
5	1	5	0.70
0.5	2	10	0.46
0.05	4	20	0.20

TABLE XIV. EFFECT OF ACTIVATION ENERGY ON REACTION RATE

Activation Energy (cal/mole)	Linear Reaction Rate (cm/sec)
15,000	0.97
20,000	0.69
25,000	0.50
30,000	0.34
35,000	0.12

Several refinements are available in the program which are designed to describe actual physical characteristics and reaction phenomena more precisely.

(1) Effect of Particle Shape

Figure 1 and scanning electron micrographs show that metallic particles come in different shapes - some spherical, others like platelettes. The computer program used in this study assumes that the particles A and B, described on page 25, are infinite plates of effective thickness Ψ . Another program described spherical particles A of diameter Ψ to have been immersed in a continuous matrix of B. The numerical difference in output data was not sufficiently large from those obtained from the parallel plate model to require a correction of the program presented in this report.

(2) Effect of Particle Size Distribution

The program permits the specification of 15 particle sizes, each assigned with a measured statistical frequency. Usually, the effect of particle size distributions is small if the distribution is narrow. The effect of a large fraction of larger particles is to act in the reaction zone as a diluent. An experimental and analytical study of diluents has shown that such systems have a lower reaction temperature, and because of corresponding lower diffusivities, have slower reaction rates. Large particles have the effect of increasing ignition times, energies, and delays. These matters will be discussed in Section IV.

(3) Effect of Phase Changes

The computer program allows for a phase change in the lower melting constituent. If a phase change occurs in a system of stoichiometric proportions, no effect on performance is observed. If the phase change occurs in a diluent or in a reagent which is present in excess, a phase change acts against the reaction by lowering the reaction temperature.

(4) Effect of Changes in Composition

As illustrated on page 25, changes in composition are handled by the computer program through the selection of appropriate diffusion barrier thicknesses which arise from particle size and the weight fraction of the individual constituents.

(5) Effect of Changes in Reaction Mechanism and Properties

This program is designed to describe intermetallic and other condensed phase reactions during the ignition phase and assumes that a single diffusion rate law can describe the process. When other species or gas phases are formed as a result of the reaction, variant reaction rates must be expected because the present mathematical model makes simplifying assumptions as to the constancy of transport parameters, rates, and processes.

SECTION IV

STUDY OF IGNITION CHARACTERISTICS

1. EXPERIMENTAL STUDY

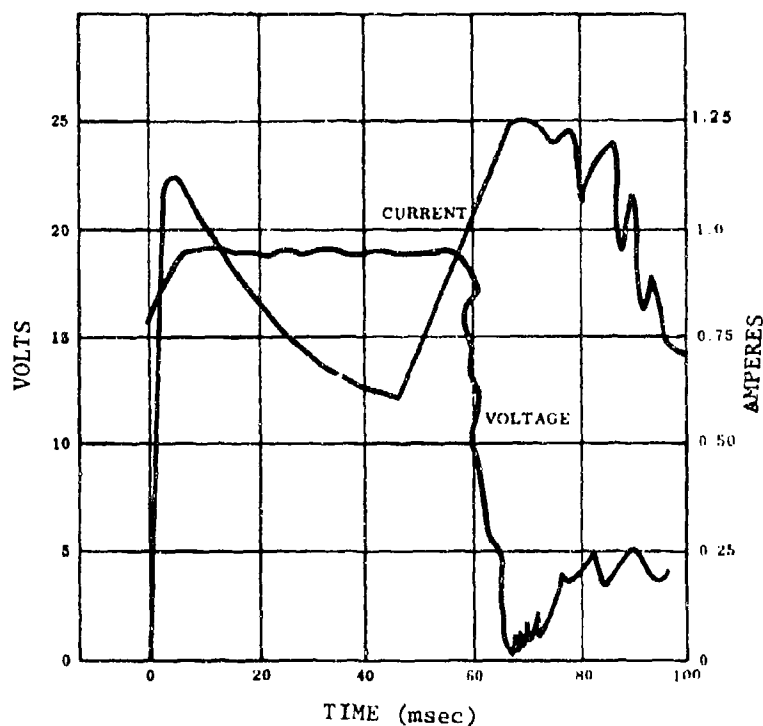
Intermetallic reactions are easily and reliably ignited by brief high-temperature events. The amount of ignition energy and the time requirement have been the subject of special emphasis in this program because of the great importance of characterizing the ignition energies in many types of pyrotechnic processes. Ignition characteristics of intermetallic reactions have been studied experimentally with first fires, ignition wires, spark discharge, and thermal flux. The common observation that condensed phase reactions are unreliable, whether thermitic or intermetallic, has been shown to be wholly caused by insufficient attention to the heat-transfer characteristics. Systems having low thermal conductance, such as those containing carbon or boron, have been shown to react so strongly as to react under water, once initiated.

In Section III it is shown that excessive thermal conduction causes quenching of the reaction. Similarly, high thermal conduction requires high ignition energies. When using a first fire or hot wire to ignite an intermetallic reaction mixture such as Ni-Al, it is necessary to deposit so much energy into the mixture that the temperature of the entire mass is raised substantially above ambient temperature. Addition of a component which reduces thermal conduction, such as boron powder, substantially reduces the amount of required ignition energy. Low thermal conductivities are therefore one of the requirements for promoting ease of ignition. For this reason, the experimental study has focused on the boron and carbon mixtures of titanium and zirconium.

Intermetallic reaction mixtures of titanium or zirconium are readily initiated with a first fire which may either be pressed as a layer on the reaction mixture or it may be poured on loosely. Studies were made using Al/V₂O₅, B/V₂O₅, B/BaCrO₄, Mg/BaCrO₄, and composites of these. The amount of first fire need not be much - large masses of a boron and carbon mixture with titanium and zirconium are reliably ignited with a small fraction of a gram of first fire which is triggered by a hot wire or an electric match. This ignition technique was not developed to the point of obtaining quantitative data.

Another measure of the ignition energy was obtained by stripping the glass casing off a flashlight bulb and immersing the tungsten filament in the reaction mixture. Reactions could be initiated within a few milliseconds using a voltage which depended on the size of the tungsten filament and also on the particle size of the mixture. For 2- μ boron mixtures with titanium, 10 to 20 V would suffice. Lower voltages would cause the ignition delay to be increased many times pointing to a possible change in ignition mechanism. High voltages of about 100 V would tend to shorten the ignition delay. The current and voltage input to the filament was recorded on an oscillograph, yielding photographic records such as those shown in

Figure 9. The ignition time (and, hence, the ignition energy) was assigned to the time at which an abrupt change in current and voltage was recorded. Such changes were ascribed to the formation of a thermally conductive reaction mixture or the burning through of the filament. This method does not necessarily yield the minimum energy, as ignition could have been initiated before the wire burned through or afterward due to the continued energy deposition into the reaction mixture from the power supply. Ignition characteristics could better be determined through controlled timing of energy deposition, or by other techniques such as laser deposition or image furnace technology. Such studies were beyond the scope of this effort.



Ignition Energy Using a No. 328 Bulb
 $18 \text{ V} \times 0.80 \text{ A} = 14.4 \text{ W}$
 $14.4 \times 50 \times 10^{-3} \text{ sec} = 0.720 \text{ J}$
 $= 0.172 \text{ cal}$

Figure 9. Ignition History of -325 Mesh Titanium-Boron Mixture

Another method for initiating intermetallic reactions was with a high voltage discharge. A feasibility demonstration was made by discharging a 2- μ f capacitance across electrodes which were inserted into a fine titanium-boron mixture. It was shown that the finer the powder mixtures, the lower was the required discharge voltage. For instance, 10- μ boron was initiated with the capacitance charged to 4000 V while a 60- μ titanium mixture was not initiated. No attempt was made to monitor the actual voltage drop across the electrodes or to measure the current of the spark. The stored energy in the above case was 16 J, with the capacitance discharging in 0.1 msec. No studies were performed on the role of thermal or electrical conductivity of the mixture on the required spark energy.

2. ANALYTICAL STUDY OF IGNITION CHARACTERISTICS

Ignition energy is a complex function of heat capacity, thermal conductance, and diffusivity. It can be expressed as energy per unit mass provided that the mass of the (adiabatically) reacting material is specified, or as energy per unit area provided that the ignition time is also specified. Both methods are illustrated in this report. The calculation of the ignition flux and ignition time by a mathematical model (p. 25) is illustrated in Appendix IV. The resulting data for various reaction mixtures are listed in Table XV and shown schematically in Figures 10 and 11. No exact experimental verification of these calculations is available, but points obtained by tungsten filament method (Figure 9) and by ignition in a filament image furnace show that the computed data are consistent with experimental observation. It should be remembered that the ignition fluxes are averaged values, explaining why the most reactive mixtures seemingly require the highest flux.

In examining the data shown in Table XV, one must envision variant ignition times and fluxes for each source temperature. This means that these data are illustrative only and they should be repeated for each ignition method. These data yield insight into the magnitude of flux required and so facilitate the design of hardware or of verification tests. Both ignition time and fluence are affected by particle size and conductance, explaining the results obtained in the high voltage discharge study.

Another way of describing ignition energies is by computing the mass of igniter required to initiate the reaction. As before, the results will be determined by conductance, diffusivity, and particle size as well as by the temperature (enthalpy) of the ignitor. The computer program for performing this calculation on a concentric cylindrical geometry is shown in Appendix III, and it is illustrated in Figure 12. The scheme is to vary the size of the igniter until the resulting enthalpy is sufficient to initiate a self-sustained reaction.

Either method, the fluence calculation or the ignition energy calculation, may be used to design hardware and to assess the safety of pyrotechnic mixtures with respect to thermal transients. Other geometries may be similarly programed, and codes can be written which calculate ignition energies directly.

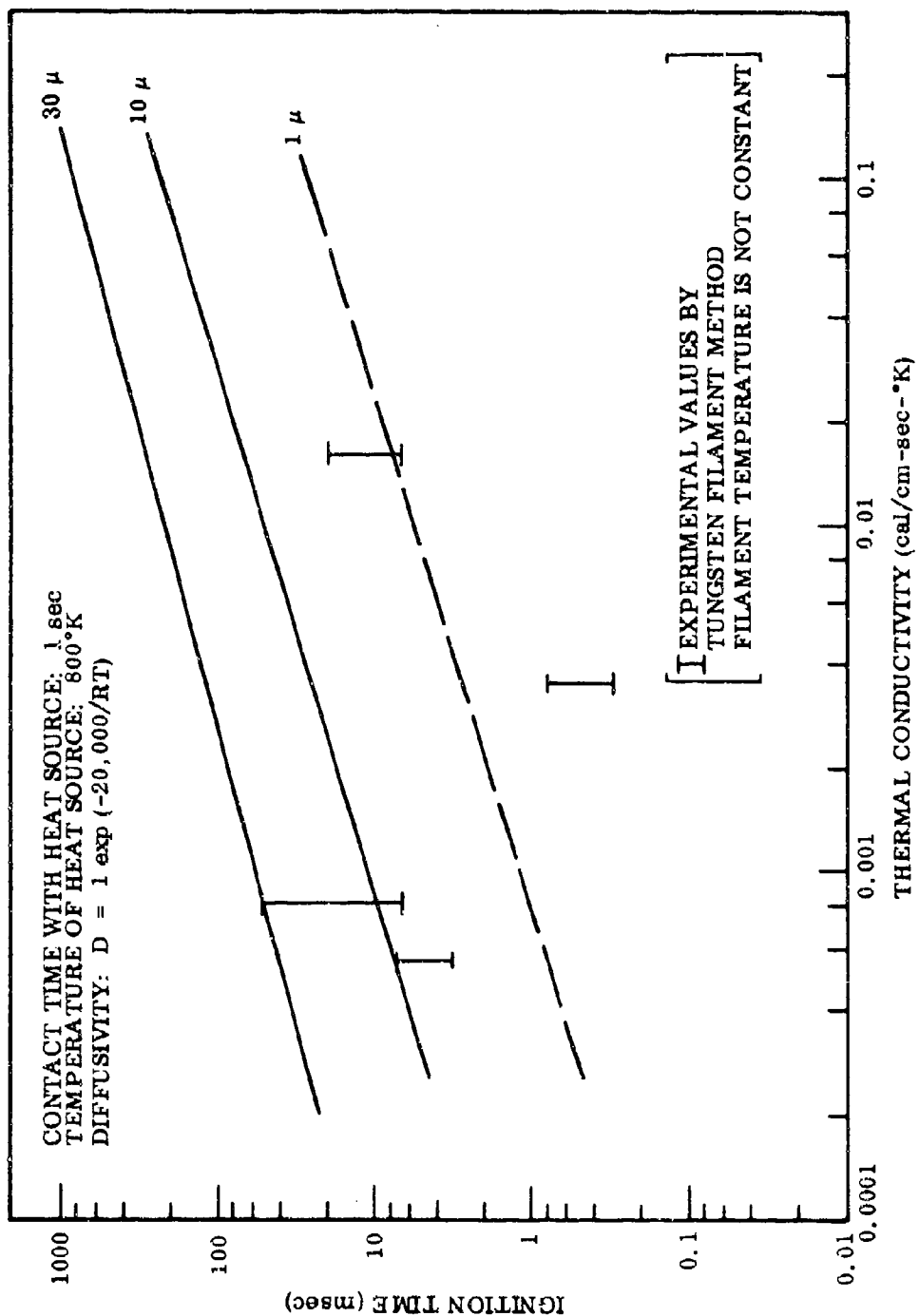


Figure 10. Computed Ignition Times of Intermetallic Reaction Mixtures

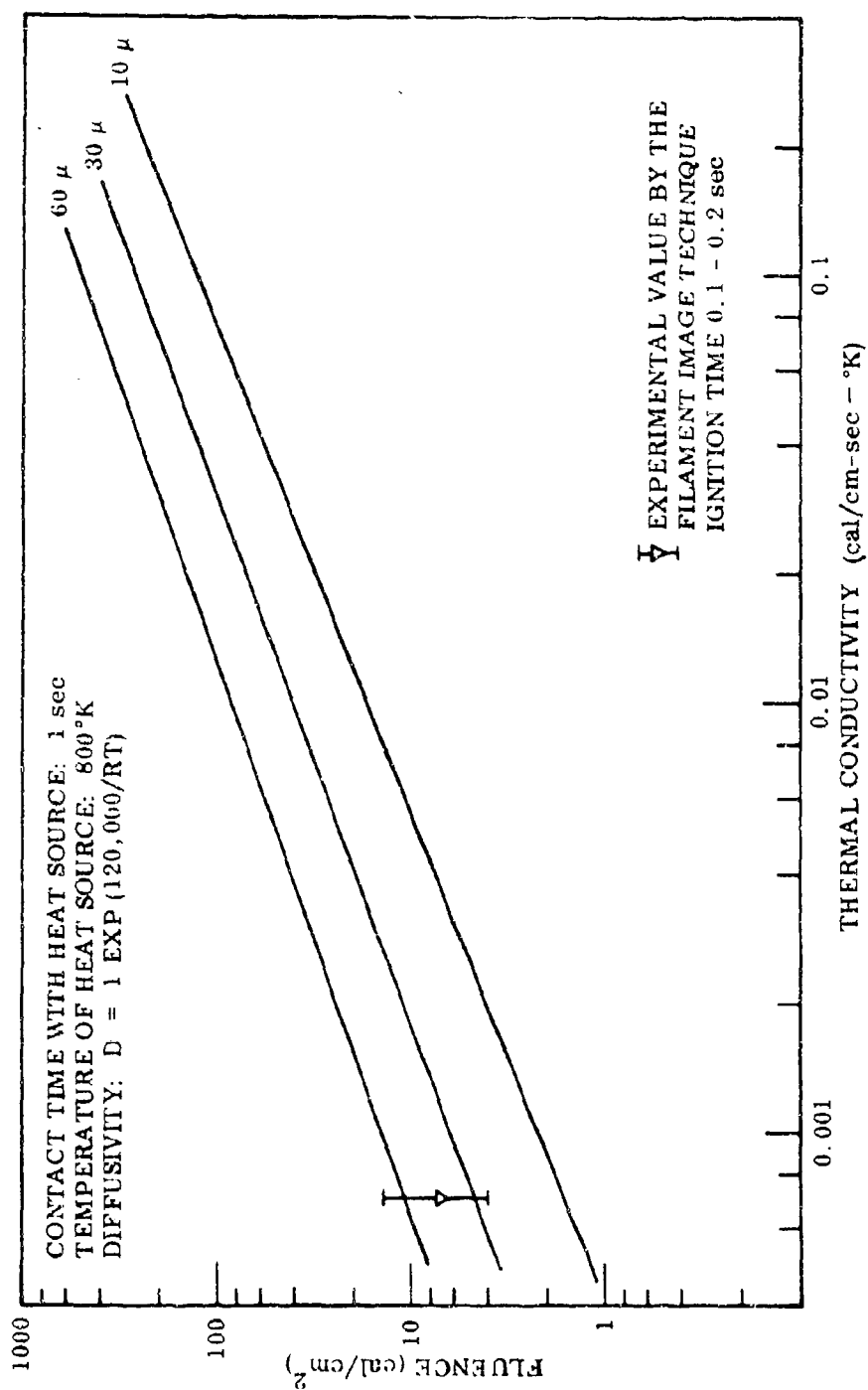


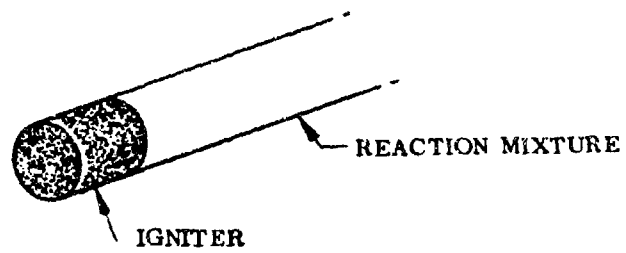
Figure 11. Computed Ignition Fluences of Intermetallic Reaction Mixtures

TABLE XV. COMPUTED IGNITION CHARACTERISTICS

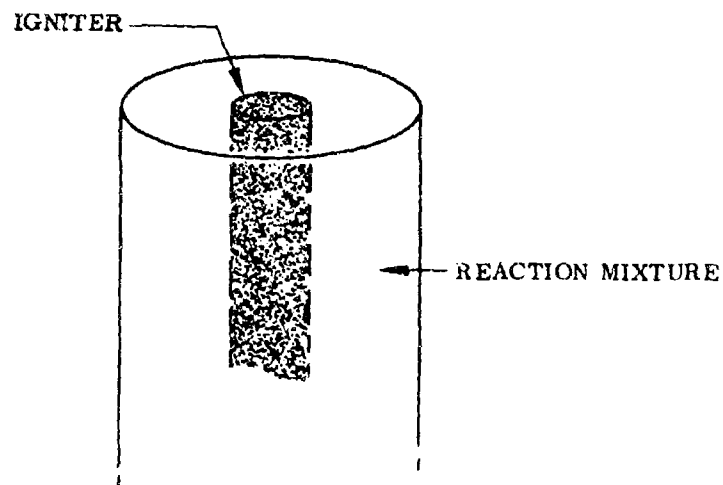
Contact Time With Heat Source: 1 sec Temperature of Heat Source: 800°K					
Thermal Conductivity	Particle Size (μ)	Ignition Energy (cal/g)	Ignition Time (msec)	Ignition Fluence (cal/cm ²)	Ignition Flux (cal/cm ² sec)
D = 1 exp (-20000/RT)					
0.00056	3	788	5.75	0.90	156
0.0008	10	3710	12	1.79	160
	30	4130	100	5.55	55.5
	60	4000	464	10.85	26.5
0.0035	3	642	7.65	3.06	400
	9	680	24	5.75	240
0.017	10	2280	14.5	6.80	470
0.054	25	5500	740	148	200
0.16	25	5900	370	190	515
D = 10 exp (-20000/RT)					
0.0008	1	700	0.21	0.01	50
	9	1640	2	0.79	400
	30	1660	19	2.4	126
	60	1300	74	3.72	51
0.0082	38	7770	320	48.2	150

As illustrated in Section III, computer modeling permits the assessment of the relative importance of the various parameters in the initiation process. Furthermore, it may serve as a tool for studying the safety of pyrotechnic mixtures toward ignition by thermal transients or spark discharge.

The analytical treatment assumes an igniter (or first fire) of known density, heat capacity, thermal conductivity, and which is brought instantaneously to a uniform ignition temperature. The temperature of the igniter then drops uniformly due to heat conduction into the intermetallic. The ignition energy was computed for an igniter of $L/D = 1$ which defines its mass, enthalpy, and surface area.



a. End Burning Ignitor



b. Internal Ignitor

Figure 12. Illustration of Mathematical Approach to the Determination of Minimum Ignition Energy

The computed ignition energies have been plotted on Figure 13 as a function of thermal diffusivity with particle size as a parameter. These data are obtained for diffusion prefix, D_0 , of $5 \text{ cm}^2/\text{sec}$ and an activation energy of 20,000 cal/mole. Actually, many systems have lower diffusivities with the result that the energies shown in Figure 13 would be expected to be higher. The data are plotted versus thermal diffusivity, $\kappa/\rho C_p$, in order to compensate for variations in density.

Figure 13 also shows experimental data for ignition energies which were determined using the tungsten filament method described in Section IV. The agreement between experimental and analytical data must be considered adequate as neither the theoretical diffusion parameters nor the actual densities of the test mixtures are known precisely.

The main observation which one would make from such a correlation is that the required ignition energies are indeed small - about 0.2 cal or 1 J for a typical titanium mixture with carbon or boron. This corresponds to less than a milligram of the typical first fire, or a diameter of an igniter cavity of less than a millimeter. That these magnitudes are correct is borne out by the success of using a fine tungsten wire as the ignition system.

Such findings have profound implications for the manner in which conventional ignition systems are used. It appears that greater reliability or a smaller ignition system would be possible if the role of thermal diffusivity in the ignition process were better appreciated. For instance, conventional thermite systems could be easily ignited if the highly conductive aluminum were encapsulated in a thermally nonconductive medium. Recent developments have shown this to be possible (45). Appendix IV describes how the computer output can be utilized in obtaining the ignition energy flux and the ignition energy.

3. APPLICATION OF IGNITION STUDIES TO INCENDIARIES

The preceding section described experimental and theoretical techniques by which the effective performance of intermetallic reactions as igniters could be determined. This section will describe briefly several demonstrations of these findings.

a. Ignition and Reaction of Thermites and Thermates

Figure 14 shows a magnesium cylinder filled with Thermate TH-3 and fitted with a tungsten filament and a Ti-2B igniter. Voltage signals of as little as 16 V from a dry cell will ignite the system within milliseconds, assuring complete combustion of the thermate. This type of device was assembled to demonstrate the potential for igniting normally sluggish reaction mixtures. The same system also works with thermite.

Figure 15 shows a large (250 g) pressed body of a Ti-2B mixture into which a 1/4-in. cavity was drilled. Into this cavity was inserted a tungsten filament Ti-2B igniter assembly. This type of system will also ignite within milliseconds as was shown by a motion picture study. The product of this reaction is a solid clinker with a fairly uniform distribution of voids. The incendiary action can be augmented by dispersion of

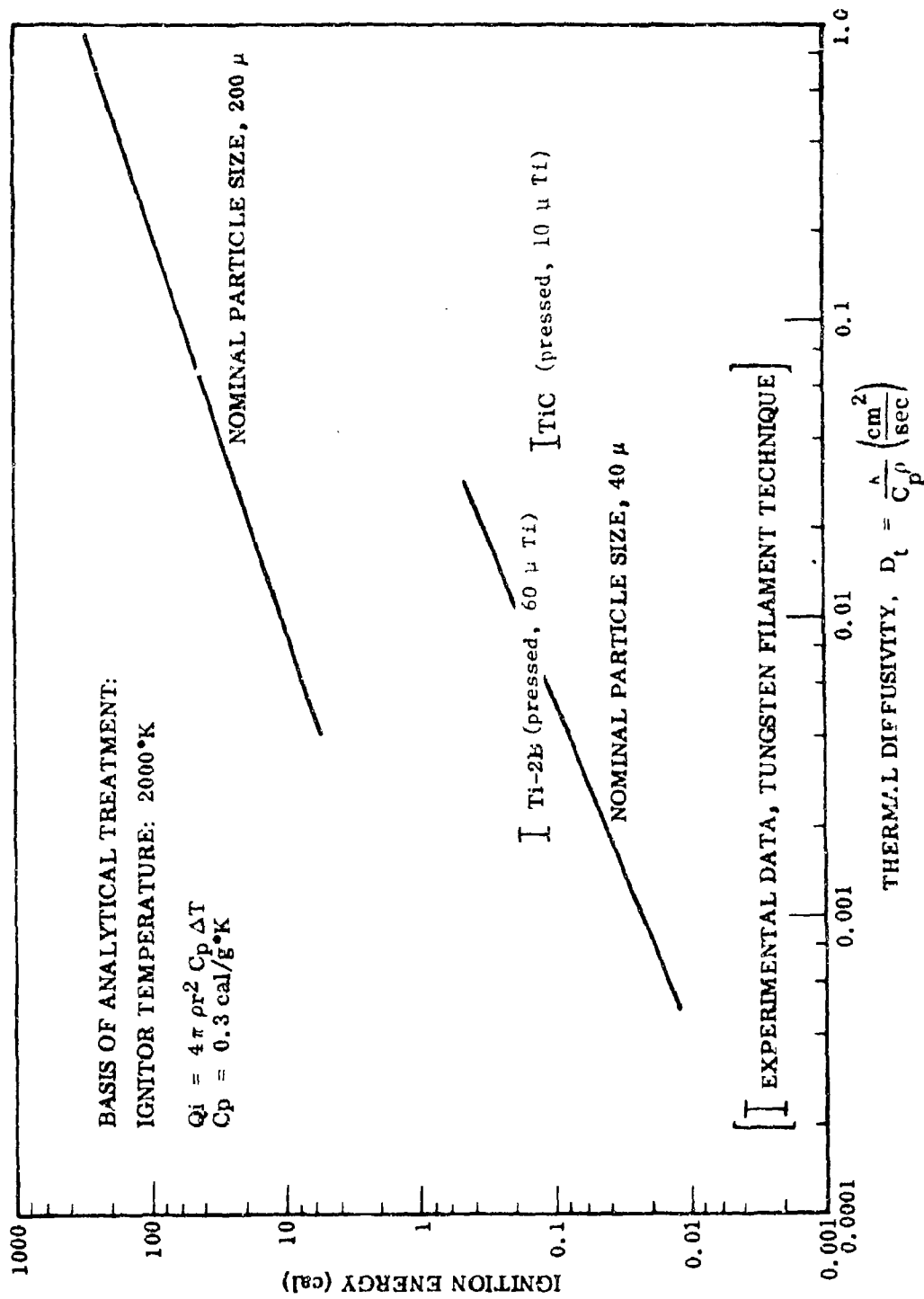


Figure 13. Ignition Energies of Intermetallic Reaction Mixtures

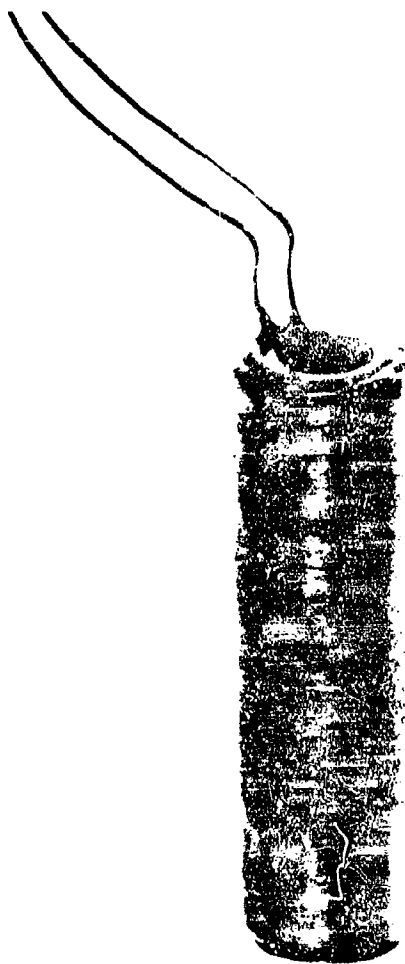


Figure 14. Assembled Incendiary Demonstration Unit

1/2 x 2 in. magnesium cup with No. 328 flash light bulb. Inserted tungsten filament is in contact with Ti-2B igniter mixture, the remaining cup filled with thermate TH-3.

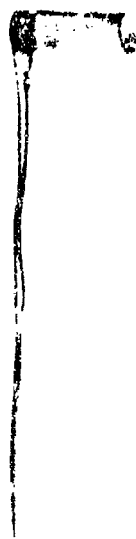
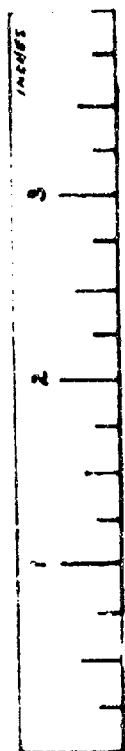


Figure 15. Titanium-Boron Reaction Mass With Intermetallic Reaction Igniter
2-1/2-in. diameter Ti-2B body, pressed to 20,000 psi. approximate weight, 250 g. Igniter consists of a No. 328 flashlight bulb with exposed tungsten filament. This filament is in contact with loosely pressed Ti-2B igniter mix.

the reacting mass. The most effective agent for breaking up large chunks of intermetallic reactants has been the addition of a thermite. An example is a mixture of Al/CuO which upon reaction generates copper vapor. This vapor is thought to be the agent responsible for the explosive action.

The high cost of intermetallic reactants may restrict these reaction mixtures to the role of igniters of the inexpensive but sluggish thermites and thermates. As shown in the preceding section, by proper control of the thermal transport characteristics of both intermetallic and thermite mixtures, greatly improved and economically attractive incendiaries can be designed.

b. Use of Intermetallic Reactions in Tracer and Incendiary Munitions

Conventional tracer munitions utilize a metallic element such as zirconium or magnesium with an oxidizer such as a chlorate, perchlorate, or nitrate. Problems relating to storability, reliability, and operational difficulties have prompted a search for alternate reagents.

A thermal analysis of intermetallic reactions showed that ignition times of the order of dwell time in the rifle (2.8 msec) and reaction times on the order of the flight time (2 sec) were feasible. Figure 16 shows the simulated temperature history of a tracer bullet which was initiated in 5 msec at 2800°K. Upon emerging from the barrel, the temperature of the exposed surface drops while the heat diffuses into the bullet. After approximately 40 msec, the temperature has risen to the steady state value. This shows it is not necessary that the reaction mixture remain exposed to the heat source until the reaction temperature has been reached but only until sufficient heat has been added to overcome the diffusion limited reaction.

Such a reaction mixture can act as a tracer component as well as a delay fuze. Upon impact, a visible signature may result. The delay fuze may ignite a pyrotechnic charge, be it a signal flare, a smoke grenade, or an incendiary. The projectile may be a bullet, armor piercing projectile, or a shaped charge.

Tests were performed on intermetallic reaction mixtures which were uncompressed. These will react with the formation of a luminous fountain. The use of such reaction mixtures as filler for shaped charges has been suggested.

The feasibility of using intermetallic reaction mixtures as igniters under transient conditions was demonstrated by the insertion of a pressed intermetallic component into a smoke cartridge. Ignition with a black powder charge was demonstrated (46) and resulted in reliable generation of smoke owing to the retention of the reaction energy by the ignition system.

c. Formulation of Intermetallic Reaction Mixtures

Preliminary tests have indicated the feasibility of formulating and shaping intermetallic reaction mixtures in a continuous manner. Addition of glues such as gum arabic and inorganic binders (45) have produced firm shapes suitable for use in

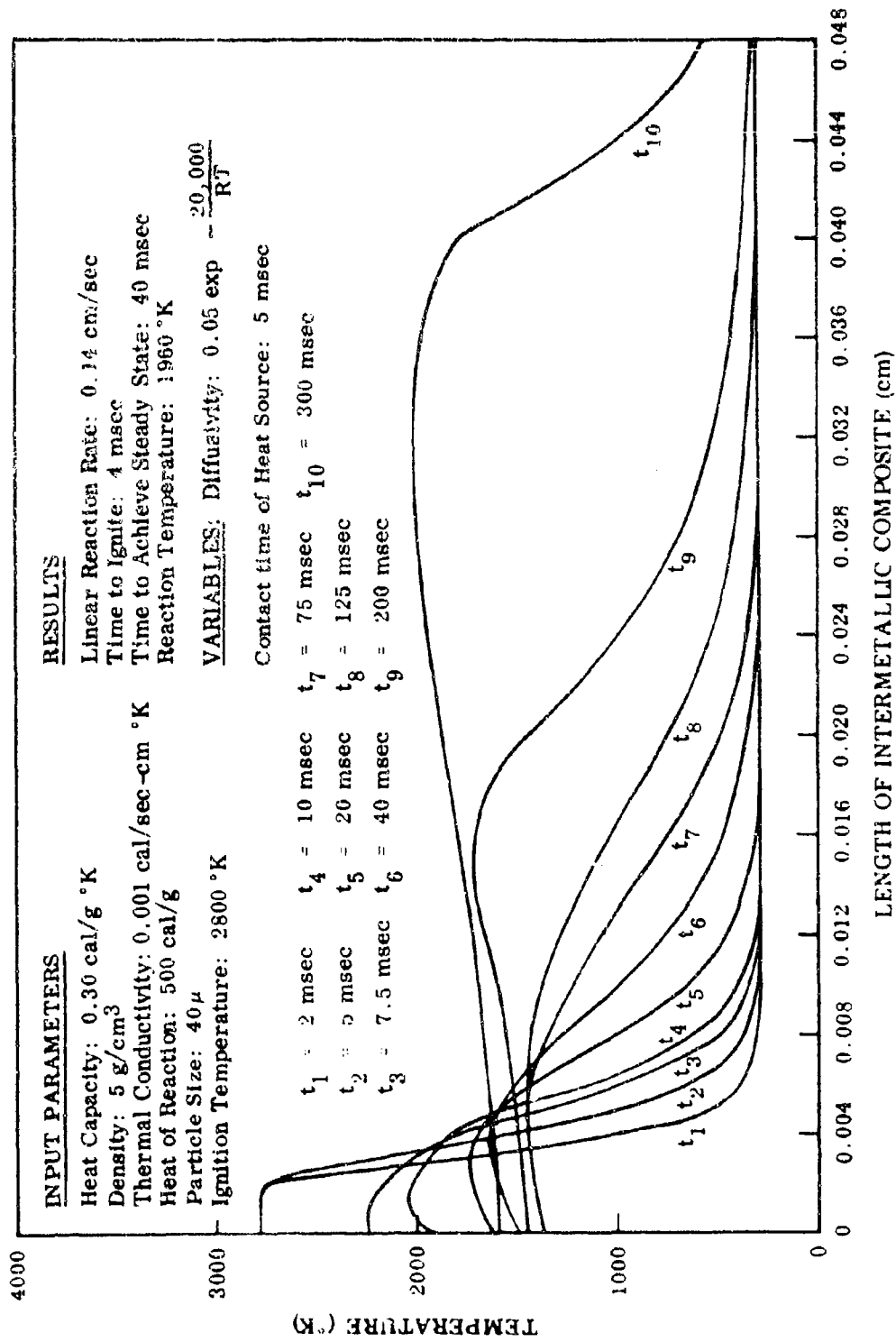


Figure 16. Computer Run of Hypothetical Intermetallic Mixture, Ignited by Transient Heat Source

igniters. A preliminary test has shown that intermetallic mixtures can be extruded as rods or tubes when these are mixed as a paste with lubricants. Fifty percent by weight of water containing 5 percent gum arabic or a similar amount of volatile organic solvent containing a small percentage of a nonvolatile binder are recommended for this purpose.

SECTION V

APPLICATION OF INTERMETALLIC REACTION TO PYROTECHNIC AND ORDNANCE TECHNOLOGY

1. CHARACTERISTICS OF INTERMETALLIC REACTIONS

This study has shown intermetallic reactions to have many characteristics which are desirable for pyrotechnic and ordnance technology. Several such characteristics have been measured and put to use in present devices; others await additional development effort.

- Shock Resistance. Mixtures of metal powders cannot be initiated by shock as by sudden compression, by dropping of a weight, by friction, or by dynamic shock. In this way they differ from pyrotechnic igniters containing chlorates or from ordnance initiators containing primary explosives.
- Temperature Resistance. Mixtures of metal powder will not be initiated at moderate temperatures.² This means that pyrotechnic components containing intermetallic reaction systems can be stored and operated at temperatures above those containing nitrates, chlorates, and other conventional oxygenators. Igniters containing intermetallic mixtures can operate beyond the stability limits of thermites.
- Corrosion Resistance. Pyrotechnic and incendiary systems containing magnesium have low storability because of the effect of moisture. Other examples are the action of the decomposition products of single and double base propellants on ordnance components. Sensitive materials now require inhibitors or mechanical barriers which lower reliability. Intermetallic reaction mixtures are not so affected.
- Moisture Resistance. Intermetallic reaction mixtures will not cake, leach out, diffuse out, or react under the influence of high humidity, moisture, solvents, or potting compounds. In this way, they differ from pyrotechnic components containing perchlorates and peroxides, thereby opening a new field for pyrotechnics development.
- Spark Resistance. While intermetallic reaction mixtures can be initiated by a sizable electrical discharge, they are not affected by the magnitude of electrical energy contained in stray rf signals, or static discharge by operator handling.

²Reaction mixtures containing the alkali metals, mercury, or low melting alloys of tin, indium, etc., are exceptions. As shown in this report, high thermal conductivity and low reaction energies make these systems undesirable.

The necessary safety requirements inherent in handling finely divided metal powders must be met, but control of electrical resistivity of the reaction mixture can be achieved without significant change in operating characteristics.

- Chemical Resistance. Intermetallic mixtures and their reactions are moderately insensitive to contaminants and variations in composition. This means that graded compositions of intermetallic reaction mixtures with other pyrotechnic components are possible. Low quality control standards with resulting low cost are permissible for many applications.
- Condensed Phase Reactions. Condensed phase reactions are not affected by environmental pressure and exposed surface area. This means that igniters for solid propellants for vacuum ignition can be made and that underwater application will not stop intermetallic reactions. Lack of gaseous products causes the heat of reaction to be confined to a small volume so that intermetallic reactions have a high energy density.
- Compatibility With Various Support Media. Intermetallic reaction mixtures of low thermal conductivity can serve as delay mixes and fuzes without being affected by heat loss through the container or mounting. It appears, subject to further testing, that intermetallic reactions can compete with existing delay mixtures, but operate more compactly, more reliably, and in a more adverse environment of shock, corrosion, or temperature.
- Flexibility in Reaction Characteristics. Reaction rates, ignition rates, and ignition times can be varied by changes in mixture characteristics. This means that a mixture can be tailored to meet specific performance requirements.

2. PRESENT APPLICATIONS OF INTERMETALLIC REACTIONS

At present, intermetallic reactions are chiefly employed for the ignition of pyrotechnic and ordnance devices.

Pyrofuze has been used for the ignition of propellants (4, 47); also, it has been studied as a delay time fuze (48).

Nickel-aluminum has been used as igniter-mixture for thermite cutting mixtures (49).

Titanium-boron inserts have been tested as igniters for M84A1 HC Smoke Cartridges (46).

3. FUTURE APPLICATION OF INTERMETALLIC REACTIONS

Better understanding of the means of controlling reaction characteristics will bring about a greatly expanded range of applications.

Intermetallic reaction mixtures are being developed as active components in tracer munitions (50) where they promise by absence of particulate reaction products to prevent jamming of the machine gun mechanism. Intermetallic reactions when used in tracer munitions and armor piercing munitions promise a visible signature upon impact. Intermetallic reactions have been mentioned for incendiary projectiles (45), as low ignition energy igniters for thermite cutters, as infrared heat sources, for in situ welding of space structures or refractory metals (51), as shock insensitive initiators of ordnance boosters, as igniters for signal markers, as active components to be ejected by shaped charges, and for delay fuzes (48). Bimetallic fibers allow the burning rate of a solid propellant to be increased without a significant decrease of specific impulse (52).

Use of intermetallic reaction mixtures in state-of-the-art thermite incendiaries will assure complete and rapid ignition with high reliability, producing an incendiary which is economical and immune to countermeasures such as physical removal from a target prior to ignition. A thermite device which is completely ignited will react regardless of the condition of the impact area which may be muddy, sandy, or soft. Reduction of the number of duds will improve the effectiveness of present incendiaries at little difference in cost.

Intermetallic reactions are completely compatible with pyrotechnic and thermite reactions which tend to disperse the powdered reaction mixture by spattering. Ignition times of thermite and thermite systems are shortened, and their rate of heat output is increased so that improved performance in visual (signal) and incendiary applications can be expected.

Recent improvements in thermite-type reaction mixtures (45) have made possible the expansion of thermite reactions to many types of incendiary, pyrotechnic, and ballistic munitions. The analytical and experimental techniques developed in this program are directly applicable to an evaluation of other pyrotechnic mixtures offering a new technique for selecting such thermal and kinetic properties as to assure successful performance of the devices with a minimum of trial-and-error testing.

SECTION VI

CONCLUSIONS AND RECOMMENDATIONS

Exothermic intermetallic reactions have been shown to be an altogether new class of pyrotechnic system. Like the well known thermite systems, they react without forming a vapor phase. The reaction rates are determined in part by diffusivity and particle size. Additional parameters which offer a possibility of control are thermal conductivity, heat of reaction, and composition.

Intermetallic reactions have been shown to be amenable to successful analysis of the heat transfer process through computer programming. This has been proven to be a powerful tool in the selection of components which will produce the desired reaction characteristics. Moreover, the techniques developed promise to be of value in analyzing the performance of other condensed phase reactions such as those of thermites.

Of particular value has been the assessment of the minimum ignition energy requirement and response delay characteristics in terms of particle size, thermal conductivity, and heat of reaction. These studies have pointed the way to a wide range of applications, ranging from utilization of intermetallic reactions in tracer munitions, as igniters for smoke cartridges and signal flares, in infrared decoys, to shock and temperature resistant boosters for ordnance systems.

Further computer studies are necessary to define ignition characteristics. It is recommended that computer-generated findings of ignition characteristics be corroborated by experimental study of intermetallic as well as thermite-type systems. Such studies should be performed using transient energy sources such as spark discharges, powder flashes, lasers, and shuttered image furnaces. It is also recommended that further pyrotechnic and ordnance applications of intermetallic reactions be tested, particularly those in need of a temperature-stable, corrosion and moisture-resistant, and shock-insensitive ignition system. The incendiary characteristics of existing devices can be improved through the use of intermetallic ignition systems.

APPENDIX I
SOURCES AND SPECIFICATIONS OF REAGENTS

Aluminum

Alcoa No. 120	Atomized	40% - 325 mesh 60% - 40 mesh	15 μ Effective Size
Alcan MD 44	Atomized	21% + 100 mesh 26% + 200 mesh 13% + 325 mesh 40% - 325 mesh	30 μ Effective Size

Nickel

Sherritt Gordon Mines Ltd., Grade F	5% + 250 mesh 40% + 325 mesh 60% - 325 mesh	40 μ Effective Size
International Nickel Co.,	Type 123 Carbonyl Nickel 4-7 μ Type 255 Carbonyl Nickel 2.6 - 3.4 μ	

Titanium

Atomergic Chemical Co., Approximately 10 μ size
 Consolidated Astronautics -30 + 100 mesh, 100 μ Effective Size
 Atlantic Equipment Engineers, -50 + 100 mesh, 60 μ Effective Size
 -200 + 325 mesh, 30 μ Effective Size
 -325 mesh, 10 μ
 10 μ , 1 μ Effective Size

Zirconium

Atomergic Chemical Co., Approximately 10 μ size
 Consolidated Astronautics, -30 + 100 mesh, 300 μ nominal size
 Foote Chemical Co., G Grade, 2 μ size, 3 μ Effective Size

Carbon

Graphite No. 41B, Consolidated Astronautics, 0.5 μ Effective Size
 Shaningan Chemical Co., Actylene Black, Agglomerates 1 μ
 Fines < 10⁻² μ

Boron

Research Grade, U.S. Borax and Chemical Co., 95% Research, Effective Size: 2 μ
 Atlantic Equipment Engineers, 90-92% Grade, Effective Particle Size: 10 μ

APPENDIX II

PROGRAM STATEMENTS FOR LINEAR RATE STUDIES

Program Description

The program performs the following operations in sequence:

- (1) Calculation of the temperature in each length increment (slice) of a rod-shaped reaction body over a series of time increments.
- (2) Calculation of the extent of reaction in each slice over a series of time increments.
- (3) Use of a measured spectrum of particle sizes in calculating the rate of diffusion and the rate of heat evolution.
- (4) Determination of the temperature rise on the basis of data on phase transitions for the low melting metal.

Input Parameters

The following data are read in:

C	heat capacity, cal/deg-g
RO	density
KT	heat conductivity, cal/cm-deg-sec
DO	preexponential factor in Arrhenius expression
E	activation energy, cal/mole
Q	heat of reaction, cal/g
EPS	emissivity (currently set at 0.9)
R	radius of rod, cm
XL	length of rod, cm
XSOFO	nominal thickness of low melting metal in mixture particle, cm
XHARO	nominal thickness of high melting metal in mixture particle, cm
THKO	nominal particle size, cm
CONS	initial concentration of low melting metal
DX	thickness of each slice (distance increment), cm, not less than THKO
FT	number of DDT in DT, chosen to be 20 (see discussion)
TEMIN	temperature of ignition source, °K
TIMIN	heating duration, sec
TO	initial temperature of sample (usually 300°K)
P	constant (around 0.10), selected to adjust magnitude of DT (see discussion)
MXT	maximum number of time increments desired
TMLT	melting point of low melting metal, °K
HFU	heat of fusion of low melting metal, cal/cm ³

Discussion of Program

The distribution of particle sizes is also specified in the input as follows. The data are made up of 15 sets of 3 numbers for 15 size increments. The first number is the normalized frequency factor for the size increment. The second is the thickness of the low-melting metal, and the third is the thickness of the high-melting metal in each particle. In this manner, variations in density and composition of the mixture constituents can be accounted for.

The first section of the program calculates certain quantities needed in subsequent computations, sets up initial conditions for temperature and for the unreacted material, and prints out the input data. In the remaining portion of the program, a complete calculation is carried out for each time increment, DT . The maximum number of these increments is specified, usually 1000.

For each time increment, heat conduction is first calculated and a tentative temperature distribution along the rod-shaped sample is obtained. Material diffusion is calculated independently. This is the most time-consuming part of the program. To calculate the extent of diffusion during a given time increment, DT is divided into a number of smaller increments, DDT . That number is determined by the program for each individual DT so that DDT is small enough to give acceptable accuracy in the diffusion calculation, yet not so small as to make the computer time too long. Usually the number of DDT in each DT is between 10 and 25.

Since the rate of reaction is assumed to be controlled by the rate of diffusion, once the extent of diffusion is calculated, it can be used directly to compute the heat evolved and the fraction of material that is still unreacted.

The diffusion calculation is carried out 15 times, once for each particle size. The heat evolved from different particle sizes is summed, using spectral coefficients as weights. Then the temperature rise due to reaction is computed.

Thermal radiation is also calculated independently. It is assumed that during each time increment, DT , the lateral surface of the slice radiates at the temperature prevailing at the beginning of DT . The heat lost by radiation is distributed uniformly throughout the volume of the slice.

The tentative temperature is now corrected for heat gain from reaction and heat loss from radiation.

After printing out the results, the program goes to the next time increment DT .

The magnitude of DX is important for the success of the run. This is because the time increment DT is calculated from it. The magnitude of DT is selected (through the equation: $DT = P * C * RO * DX **2 / KT$) so that the reaction takes place during the series of time increments specified. If DT is too short, the reaction will start only near or even after the end of this series. The velocity of the reaction front

cannot be evaluated properly if ΔT is too long because the reaction will be completed in all slices during the first few time increments. In this case, evaluation of the speed of the reaction front might not be possible and calculation of heat transfer and material diffusion might be too inaccurate. ΔX is chosen to be approximately equal to the nominal particle size.

The program statements follow.


```

1*      DIMENSION T(100,3), D(100,3), F(100,3)
2*      DIMENSION SPC(15), XSF(15), XHR(15)
3*      DIMENSION XSOF(15), XHAR(15), THK(15), SPCO(15), HOVS(15)
4*      DIMENSION THSOF(100,3,15), PRCX(100,3,15)
5*      DIMENSION SOLF(100,3)
6*      REAL KT
7*
8*      300 FORMAT(4E10,3)
9*      302 FORMAT(4E10,3,110)
10*     400 FORMAT(1H0,6H C = ,E7,2,2X,6H RO = ,E7,2,2X,6H KT = ,E7,2,2X,6H
11*     *DO = ,E7,2,2X,6H E = ,E7,2,2X,6H Q = ,E7,2,2X,6H EPS = ,E7,2,2X,6H
12*     402 FORMAT(1H ,18X,6H RADIUS,7X,6H LENGTH,6X,6H HIGH TEMP,5X,6H HIGH TIME,5X
13*     * ,9H PART SIZE,5X,6H DELTA X,7X,6H DELTA T)
14*     404 FORMAT(1H ,5X,6H ACTUAL,4X,/(E10,4,3X)/)
15*     406 FORMAT(//,14,2X,7H INDEX,4X,7HRL TIME,4X,7HRL DIST,
16*     * 3X,9H UNREACTED,3X,7HRL TEMP,5X,6H D(I,M),6X,3H DUT,8X,5H THSOF,
17*     * 6X,4H PROX/)
18*     408 FORMAT(1H ,3X,14,5X,E9,4,4X,14,3X,8(2X,E9,4))
19*     410 FORMAT(1H ,18X,6H SOFLAY,7X,6H HARLAY,6X,6H SOF CONS,5X,6H RATIO,5X
20*     * ,9H ROOMTEMP,4X,6HFT INPUT,6X,6H MAXTIM)
21*     412 FORMAT(1H ,9X,6H ACTUAL,4X,6(E10,4,3X),114)
22*     420 FORMAT(1H0,26X,4H SPCO,15X,4H XSOF,15X,4H XHAR,15X,3H THK)
23*     422 FORMAT(1H0,20X,4(E10,4,10X))
24*     430 FORMAT(16)
25*     432 FORMAT(6E10,4)
26*     434 FORMAT(1H0,5X,16H MELTING POINT = ,F10,1,2X,8H DEGREE K,5X,
27*     * 17H HEAT OF FUSION = ,F10,1,2X,9H CAL/CM**3)
28*     READ(5,432) (SPC(I), XSF(I), XHR(I), I=1,15)
29*     KASE = 0
30*     200 KASE = KASE+1
31*     IF(KASE .EQ. 1) WRITE(6,440)
32*     440 FORMAT(1H1,10HTIME2 30 MU)
33*     IF(KASE .EQ. 2) WRITE(6,442)
34*     442 FORMAT(1H1,10HTIME2 60 MU)
35*     READ(5,300) C, RO, KT, DO, E, Q, EPS
36*     READ(5,302) R, XL, XSOF, XHAR, THK, CONS, DX, FT
37*     READ(5,302) TEMIN, TIMIN, TO, P, MXT
38*     READ(5,302) TMLT, HFU
39*
40*     C
41*     C
42*     C
43*     C
44*     C
45*     C
46*     C
47*     C
48*     C
49*     C
50*     C
51*     C
52*     C
53*     C
54*     C
55*     C
56*     C
57*     C
58*     C
59*     C
60*     C
61*     C
62*     C
63*     C
64*     C
65*     C
66*     C
67*     C
68*     C
69*     C
70*     C
71*     C
72*     C
73*     C
74*     C
75*     C
76*     C
77*     C
78*     C
79*     C
80*     C
81*     C
82*     C
83*     C
84*     C
85*     C
86*     C
87*     C
88*     C
89*     C
90*     C
91*     C
92*     C
93*     C
94*     C
95*     C
96*     C
97*     C
98*     C
99*     C
100*    C
101*    C
102*    C
103*    C
104*    C
105*    C
106*    C
107*    C
108*    C
109*    C
110*    C
111*    C
112*    C
113*    C
114*    C
115*    C
116*    C
117*    C
118*    C
119*    C
120*    C
121*    C
122*    C
123*    C
124*    C
125*    C
126*    C
127*    C
128*    C
129*    C
130*    C
131*    C
132*    C
133*    C
134*    C
135*    C
136*    C
137*    C
138*    C
139*    C
140*    C
141*    C
142*    C
143*    C
144*    C
145*    C
146*    C
147*    C
148*    C
149*    C
150*    C
151*    C
152*    C
153*    C
154*    C
155*    C
156*    C
157*    C
158*    C
159*    C
160*    C
161*    C
162*    C
163*    C
164*    C
165*    C
166*    C
167*    C
168*    C
169*    C
170*    C
171*    C
172*    C
173*    C
174*    C
175*    C
176*    C
177*    C
178*    C
179*    C
180*    C
181*    C
182*    C
183*    C
184*    C
185*    C
186*    C
187*    C
188*    C
189*    C
190*    C
191*    C
192*    C
193*    C
194*    C
195*    C
196*    C
197*    C
198*    C
199*    C
200*    C
201*    C
202*    C
203*    C
204*    C
205*    C
206*    C
207*    C
208*    C
209*    C
210*    C
211*    C
212*    C
213*    C
214*    C
215*    C
216*    C
217*    C
218*    C
219*    C
220*    C
221*    C
222*    C
223*    C
224*    C
225*    C
226*    C
227*    C
228*    C
229*    C
230*    C
231*    C
232*    C
233*    C
234*    C
235*    C
236*    C
237*    C
238*    C
239*    C
240*    C
241*    C
242*    C
243*    C
244*    C
245*    C
246*    C
247*    C
248*    C
249*    C
250*    C
251*    C
252*    C
253*    C
254*    C
255*    C
256*    C
257*    C
258*    C
259*    C
260*    C
261*    C
262*    C
263*    C
264*    C
265*    C
266*    C
267*    C
268*    C
269*    C
270*    C
271*    C
272*    C
273*    C
274*    C
275*    C
276*    C
277*    C
278*    C
279*    C
280*    C
281*    C
282*    C
283*    C
284*    C
285*    C
286*    C
287*    C
288*    C
289*    C
290*    C
291*    C
292*    C
293*    C
294*    C
295*    C
296*    C
297*    C
298*    C
299*    C
300*    C
301*    C
302*    C
303*    C
304*    C
305*    C
306*    C
307*    C
308*    C
309*    C
310*    C
311*    C
312*    C
313*    C
314*    C
315*    C
316*    C
317*    C
318*    C
319*    C
320*    C
321*    C
322*    C
323*    C
324*    C
325*    C
326*    C
327*    C
328*    C
329*    C
330*    C
331*    C
332*    C
333*    C
334*    C
335*    C
336*    C
337*    C
338*    C
339*    C
340*    C
341*    C
342*    C
343*    C
344*    C
345*    C
346*    C
347*    C
348*    C
349*    C
350*    C
351*    C
352*    C
353*    C
354*    C
355*    C
356*    C
357*    C
358*    C
359*    C
360*    C
361*    C
362*    C
363*    C
364*    C
365*    C
366*    C
367*    C
368*    C
369*    C
370*    C
371*    C
372*    C
373*    C
374*    C
375*    C
376*    C
377*    C
378*    C
379*    C
380*    C
381*    C
382*    C
383*    C
384*    C
385*    C
386*    C
387*    C
388*    C
389*    C
390*    C
391*    C
392*    C
393*    C
394*    C
395*    C
396*    C
397*    C
398*    C
399*    C
400*    C
401*    C
402*    C
403*    C
404*    C
405*    C
406*    C
407*    C
408*    C
409*    C
410*    C
411*    C
412*    C
413*    C
414*    C
415*    C
416*    C
417*    C
418*    C
419*    C
420*    C
421*    C
422*    C
423*    C
424*    C
425*    C
426*    C
427*    C
428*    C
429*    C
430*    C
431*    C
432*    C
433*    C
434*    C
435*    C
436*    C
437*    C
438*    C
439*    C
440*    C
441*    C
442*    C
443*    C
444*    C
445*    C
446*    C
447*    C
448*    C
449*    C
450*    C
451*    C
452*    C
453*    C
454*    C
455*    C
456*    C
457*    C
458*    C
459*    C
460*    C
461*    C
462*    C
463*    C
464*    C
465*    C
466*    C
467*    C
468*    C
469*    C
470*    C
471*    C
472*    C
473*    C
474*    C
475*    C
476*    C
477*    C
478*    C
479*    C
480*    C
481*    C
482*    C
483*    C
484*    C
485*    C
486*    C
487*    C
488*    C
489*    C
490*    C
491*    C
492*    C
493*    C
494*    C
495*    C
496*    C
497*    C
498*    C
499*    C
500*    C
501*    C
502*    C
503*    C
504*    C
505*    C
506*    C
507*    C
508*    C
509*    C
510*    C
511*    C
512*    C
513*    C
514*    C
515*    C
516*    C
517*    C
518*    C
519*    C
520*    C
521*    C
522*    C
523*    C
524*    C
525*    C
526*    C
527*    C
528*    C
529*    C
530*    C
531*    C
532*    C
533*    C
534*    C
535*    C
536*    C
537*    C
538*    C
539*    C
540*    C
541*    C
542*    C
543*    C
544*    C
545*    C
546*    C
547*    C
548*    C
549*    C
550*    C
551*    C
552*    C
553*    C
554*    C
555*    C
556*    C
557*    C
558*    C
559*    C
560*    C
561*    C
562*    C
563*    C
564*    C
565*    C
566*    C
567*    C
568*    C
569*    C
570*    C
571*    C
572*    C
573*    C
574*    C
575*    C
576*    C
577*    C
578*    C
579*    C
580*    C
581*    C
582*    C
583*    C
584*    C
585*    C
586*    C
587*    C
588*    C
589*    C
590*    C
591*    C
592*    C
593*    C
594*    C
595*    C
596*    C
597*    C
598*    C
599*    C
600*    C
601*    C
602*    C
603*    C
604*    C
605*    C
606*    C
607*    C
608*    C
609*    C
610*    C
611*    C
612*    C
613*    C
614*    C
615*    C
616*    C
617*    C
618*    C
619*    C
620*    C
621*    C
622*    C
623*    C
624*    C
625*    C
626*    C
627*    C
628*    C
629*    C
630*    C
631*    C
632*    C
633*    C
634*    C
635*    C
636*    C
637*    C
638*    C
639*    C
640*    C
641*    C
642*    C
643*    C
644*    C
645*    C
646*    C
647*    C
648*    C
649*    C
650*    C
651*    C
652*    C
653*    C
654*    C
655*    C
656*    C
657*    C
658*    C
659*    C
660*    C
661*    C
662*    C
663*    C
664*    C
665*    C
666*    C
667*    C
668*    C
669*    C
670*    C
671*    C
672*    C
673*    C
674*    C
675*    C
676*    C
677*    C
678*    C
679*    C
680*    C
681*    C
682*    C
683*    C
684*    C
685*    C
686*    C
687*    C
688*    C
689*    C
690*    C
691*    C
692*    C
693*    C
694*    C
695*    C
696*    C
697*    C
698*    C
699*    C
700*    C
701*    C
702*    C
703*    C
704*    C
705*    C
706*    C
707*    C
708*    C
709*    C
710*    C
711*    C
712*    C
713*    C
714*    C
715*    C
716*    C
717*    C
718*    C
719*    C
720*    C
721*    C
722*    C
723*    C
724*    C
725*    C
726*    C
727*    C
728*    C
729*    C
730*    C
731*    C
732*    C
733*    C
734*    C
735*    C
736*    C
737*    C
738*    C
739*    C
740*    C
741*    C
742*    C
743*    C
744*    C
745*    C
746*    C
747*    C
748*    C
749*    C
750*    C
751*    C
752*    C
753*    C
754*    C
755*    C
756*    C
757*    C
758*    C
759*    C
760*    C
761*    C
762*    C
763*    C
764*    C
765*    C
766*    C
767*    C
768*    C
769*    C
770*    C
771*    C
772*    C
773*    C
774*    C
775*    C
776*    C
777*    C
778*    C
779*    C
780*    C
781*    C
782*    C
783*    C
784*    C
785*    C
786*    C
787*    C
788*    C
789*    C
790*    C
791*    C
792*    C
793*    C
794*    C
795*    C
796*    C
797*    C
798*    C
799*    C
800*    C
801*    C
802*    C
803*    C
804*    C
805*    C
806*    C
807*    C
808*    C
809*    C
810*    C
811*    C
812*    C
813*    C
814*    C
815*    C
816*    C
817*    C
818*    C
819*    C
820*    C
821*    C
822*    C
823*    C
824*    C
825*    C
826*    C
827*    C
828*    C
829*    C
830*    C
831*    C
832*    C
833*    C
834*    C
835*    C
836*    C
837*    C
838*    C
839*    C
840*    C
841*    C
842*    C
843*    C
844*    C
845*    C
846*    C
847*    C
848*    C
849*    C
850*    C
851*    C
852*    C
853*    C
854*    C
855*    C
856*    C
857*    C
858*    C
859*    C
860*    C
861*    C
862*    C
863*    C
864*    C
865*    C
866*    C
867*    C
868*    C
869*    C
870*    C
871*    C
872*    C
873*    C
874*    C
875*    C
876*    C
877*    C
878*    C
879*    C
880*    C
881*    C
882*    C
883*    C
884*    C
885*    C
886*    C
887*    C
888*    C
889*    C
890*    C
891*    C
892*    C
893*    C
894*    C
895*    C
896*    C
897*    C
898*    C
899*    C
900*    C
901*    C
902*    C
903*    C
904*    C
905*    C
906*    C
907*    C
908*    C
909*    C
910*    C
911*    C
912*    C
913*    C
914*    C
915*    C
916*    C
917*    C
918*    C
919*    C
920*    C
921*    C
922*    C
923*    C
924*    C
925*    C
926*    C
927*    C
928*    C
929*    C
930*    C
931*    C
932*    C
933*    C
934*    C
935*    C
936*    C
937*    C
938*    C
939*    C
940*    C
941*    C
942*    C
943*    C
944*    C
945*    C
946*    C
947*    C
948*    C
949*    C
950*    C
951*    C
952*    C
953*    C
954*    C
955*    C
956*    C
957*    C
958*    C
959*    C
960*    C
961*    C
962*    C
963*    C
964*    C
965*    C
966*    C
967*    C
968*    C
969*    C
970*    C
971*    C
972*    C
973*    C
974*    C
975*    C
976*    C
977*    C
978*    C
979*    C
980*    C
981*    C
982*    C
983*    C
984*    C
985*    C
986*    C
987*    C
988*    C
989*    C
990*    C
991*    C
992*    C
993*    C
994*    C
995*    C
996*    C
997*    C
998*    C
999*    C
1000*   C

```

```

59* C TEMIN = IGNITION TEMPERATURE
60* C TIMIN = IGNITION TIME
61* C MXT = MAXIMUM NUMBER OF TIME INCREMENTS
62* C SPCO = COEFFICIENT OF SIZE DISTRIBUTION
63* C THKO = NOMINAL PARTICLE SIZE
64* C
65* VSECT = 3.14159*R**2*DX
66* ALATS = 6.2851R*RO*DX
67* AENNS = 3.14159*R**2
68* SGMEPS = 1.37E-12*EPS
69* NL = IFIX(XL/DX)
70* IF(XL/DX = FLOAT(NL),GT, 0.5) NL=NL+1
71* NL = NL+2
72* NLM = NL-1
73* DO 136 I=1,15
74* THK(I)=XSOF(I)*XHAR(I)
75* HOVS(I)=XHAR(I)/XSOF(I)
76* 136 CONTINUE
77* PROXO = 5.0E-08
78* DT = P*C*RO*DX**2/KT
79* IGTIM = IFIX(TIMIN/DT)
80* IF(TIMIN.LT. DT) IGTIM = 1
81* HFU = HFU*XSOF/(XSOF+XHAR)
82* C
83* C INITIALIZE T(I,1) AND F(I,1) IN THE SECTIONS
84* C F(I,1) AND F(NL,1) WILL NOT BE NEEDED
85* T(I,1) = TEMIN
86* DO 100 I=2,NL
87* T(I,1) = T0
88* F(I,1) = 1.0
89* SOLF(I,1) = 1.0
90* 100 CONTINUE
91* C
92* C INITIALIZE THSOF(I,1,L) AND PROX(I,1,L) IN THE SECTIONS
93* DO 102 I=2,NLM
94* DO 138 L=1,15
95* THSOF(I,1,L) = XSOF(L)
96* PROX(I,1,L) = PROXO
97* 138 CONTINUE
98* 102 CONTINUE
99* WRITE (6,400) C,RO,KT,DO,E,G,EPS
100* WRITE (6,402)
101* WRITE(6,404)R,XL,TEMIN,TIMIN,THKO,DX,DT
102* WRITE(6,410)
103* WRITE(6,412) XSOF,XHAR,CONS,P,T0,FT,MXT
104* WRITE(6,434) TMLT, HFU
105* WRITE(6,420)
106* DO 140 L=1,15
107* WRITE(6,422) SPCO(L),XSOF(L),XHAR(L),THK(L)
108* 140 CONTINUE
109* C
110* C START CALCULATION, THERMAL CONDUCT. IS INDEPENDENT OF TEMP.
111* C START DO LOOP FOR TIME INDEX J
112* DO 116 J=1,MXT
113* C M AND N TAKE UP VALUES 1,2 AND 3 CALCULATED FROM J
114* M = MOD(J,3) + 1
115* N = MOD(J,3)+1
116* C DO LOOPS FOR SECTIONS OF ROD

```

```

117* C   DIFFUSION COEFFICIENTS CHANGE WITH J AND I BUT NOT WITH K
118* DO 148 I=2,NLM
119* DO 148 L = 1,15
120* IF(THSOF(I,N,L) .NE. 0.0) GO TO 132
121* THSOF(I,M,L) = 0.0
122* PROX(I,M,L) = THK(L)
123* GO TO 148
124* 132 D(I,N) = D0*EXP(-E/2./T(I,N))
125* KN = 0
126* DDT = DT/FT
127* 134 KN = KN+1
128* DDT = DDT/KN
129* TAM = D(I,M)*DDT/PROX(I,N,L)
130* IF(TAM .GT. 0.5*THSOF(I,M,L) .AND. DT/DDT .LT. 25.) GO TO 134
131* THSOF(I,M,L) = THSOF(I,N,L)
132* PROX(I,M,L) = PROX(I,N,L)
133* KFT = IFIX(DT/DDT)
134*
135* C   MATERIAL DIFFUSION DURING EACH DT
136* DO 124 JL = 2, KFT
137* TAM = D(I,M)*DDT/PROX(I,M,L)
138* THSOF(I,M,L) = THSOF(I,M,L)+TAM
139* IF(THSOF(I,M,L) .LT. 0.0) THSOF(I,M,L) = 0.0
140* PROX(I,M,L) = PROX(I,M,L)+TAM*(1. + HOVS(L))
141* IF(PROX(I,M,L) .GT. THK(L)) PROX(I,M,L) = THK(L)
142* IF(THSOF(I,M,L) .GT. 1.0E+06*XSOF(L)) GO TO 124
143* THSOF(I,M,L) = 0.0
144* PROX(I,M,L) = THK(L)
145* GO TO 148
146* 124 CONTINUE
147* 148 CONTINUE
148*
149* C   CALCULATE F(I,M) AND CHANGE IN P(I,M)
150* SXSOFF=0.0
151* STHSOF=0.0
152* DO 142 L = 1,15
153* STHSOF = STHSOF+SPCO(L)*THSOF(I,M,L)
154* SXSOFF = SXSOFF+SPCO(L)*XSOF(L)
155* 142 CONTINUE
156* F(I,M) = STHSOF/SXSOFF
157* DELF = F(I,M)-F(I,N)
158*
159* C   CALCULATE HEAT EVOLUTION (CAL/CM**3)
160* HEV = -DELF*(RO*Q + (1.0-SOLF(I,N))*HFU)
161*
162* C   CALCULATE HEAT RADIATION (CAL/CM**3)
163* IF(I .EQ. 2) GO TO 114
164* IF(I .EQ. NLM) GO TO 120
165* GO TO 118
166* 114 IF(UTIGTIM) 118,118,120
167* 118 HRA = ALATS*SGMEPS*(T(I,N)**4 - TO**4)
168* GO TO 116
169* 120 HRA = (ALATS+AENDS)*SGMEPS*(T(I,N)**4 - TO**4)
170* 116 HRA = HRA*DT/VSECT
171* DELH = HEV + HRA
172*
173* C   CALCULATE HEAT CONDUCTION INDEPENDENTLY OF RADIATION AND REACTION
174* 144 T(I,N) = P*(T(I+1,N)+T(I-1,N))-(2.*P-1.)*T(I,N)

```

NOT REPRODUCIBLE

```

175* C READJUST TEMPERATURE FOR RADIATION AND REACTION
176* 146 T(I,M) = T(I,M) + DEL4/C/RO
177* TTAM = T(I,N)
178* IF(F(I,M) .LT. 1.0E-05) GO TO 108
179* IF(TTAM-T(I,M)) 162,164,166
180* 164 SOLF(I,M) = SOLF(I,N)
181* GO TO 108
182* 162 IF(T(I,M) .LE. TMLT) GO TO 164
183* HFM = (T(I,M)-TMLT)*C*RO
184* HFMT = HFU*F(I,M)*SOLF(I,N)
185* IF(HFM .GE. HFMT) GO TO 168
186* SOLF(I,M) = SOLF(I,N)*(1.0-HFM/HFMT)
187* T(I,M) = TMLT
188* GO TO 108
189* 168 SOLF(I,M) = 0.0
190* HFM = HFMT-HFMT
191* T(I,M) = TMLT+HFM/C/RO
192* GO TO 108
193* 166 IF(TTAM .GT. TMLT) GO TO 170
194* SOLF(I,M) = SOLF(I,N)
195* GO TO 108
196* 170 IF(T(I,M) .LT. TMLT) GO TO 172
197* SOLF(I,M) = SOLF(I,N)
198* GO TO 108
199* 172 HRE = (TMLT-T(I,M))*C*RO
200* HSLT = HFU*F(I,M)*(1.0-SOLF(I,N))
201* IF(HRE .GE. HSLT) GO TO 174
202* T(I,M) = TMLT
203* SOLF(I,M) = SOLF(I,N) + (1.0-SOLF(I,N))*HRE/HSLT
204* GO TO 108
205* 174 T(I,M) = TMLT+(HRE-HSLT)/C/RO
206* SOLF(I,M) = 1.0
207* 108 CONTINUE
208* C
209* C BOUNDARY CONDITIONS
210* T(1,M) = TEMIN
211* IF(J .GT. IGTIM) T(1,M) = T(3,M)
212* T(NL,M) = T(NL-2,M)
213* C
214* C FOR PRINTOUT PATTERN
215* IF(J .LE. 100 .AND. MOD(J,10) .EQ. 0) GO TO 126
216* IF(J .LE. 50 .AND. MOD(J,5) .EQ. 0) GO TO 126
217* IF(J .LE. 10 .AND. MOD(J,1) .EQ. 0) GO TO 126
218* IF(J .EQ. 1) GO TO 126
219* IF(J .LE. 800 .AND. MOD(J,800) .EQ. 0) GO TO 126
220* *ERROR* THE NON ARITHMETIC STATEMENT IS MISPELLED.
221* IF(J .GT. 800 .AND. MOD(J,50) .EQ. 0) GO TO 126
222* GO TO 106
223* C HEADING FOR PRINTOUT OF ARRAYS
224* 126 WRITE(6,406)
225* DO 128 I=2,NLM
226* TIME = J*DT
227* DIST = (FLOAT(I) - 1.5)*DX
228* II = I-1
229* WRITE(6,408) J, TIME, II, DIST, F(I,M), T(I,M), D(I,M),HRA
230* 128 CONTINUE
231* 106 CONTINUE
232* GO TO 20
233* END

```

APPENDIX III

PROGRAM STATEMENTS FOR ANALYTICAL IGNITION ENERGY STUDY

Program Description

The program handles a cylindrical geometry where the ignition source is a cylinder concentric with a cylindrical reaction mass.

The distance increments are the equal thicknesses of concentric shells around the igniter while the radius of the cylinder is the counterpart of the sample length of the program described in Appendix II.

The igniter may consist of a single distance increment. If so, its radius and volume can be varied by varying DX. Alternately, the igniter may comprise a specified number of cylindrical shells so that its radius can be varied independently of DX.

The input procedure is the same as shown in Appendix II. The form of output is also the same.

This program does not handle the problem of particle size distribution; rather it calculates material diffusion on the basis of a single particle size. This particle size is the same as the nominal particle size given in the input for the other program and corresponds to the most probable particle size in the measured distribution.

Phase transition is not taken into account as it was in the program for linear rate studies on intermetallic reactions.

Thus, the list of data for this program does not include the distribution of particle sizes, the melting point for the low melting metal, or the heat of fusion.

The program statements follow.


```

60*      TIMEF = 2.*Q*DO/(C*E*XSOF**2)
61*      DISTF = SQRT(2.*A*DO*RO/(KT*E*XSOF**2))
62*      GAMMA = 2.*Q/C/E
63*      LAMDA = 0.0
64*      C      INITIALIZE T(I,1) AND F(I,1) IN THE SECTIONS
65*      C      F(I,1) AND F(NL,1) WILL NOT BE NEEDED
66*      DO 100 I=1,NL
67*      T(I,1) = TO
68*      IF(I.EQ. 1) T(I,1) = TEMIN
69*      100 CONTINUE
70*      F(I,1) = 0.0
71*      DO 102 I=2,NLM
72*      F(I,1) = 1.0
73*      THSOF(I,1) = XSOF
74*      PROX(I,1) = PROX0
75*      102 CONTINUE
76*      WRITE (6,400) C,RO,KT,DO,E,Q,EPS
77*      WRITE (6,402)
78*      WRITE (6,404) R, XL, TEMIN, X1, THK, DX, DT
79*      WRITE (6,410)
80*      WRITE (6,412) XSOF, XHAR, CONS, P, KT1, FT, HXT
81*      WRITE (6,416) TEMPF, TIMEF, DISTF
82*      WRITE (6,418) GAMMA, LAMDA
83*      C      START CALCULATION. THERMAL CONDUCT. IS INDEPENDENT OF TEMP.
84*      C      START DO LOOP FOR TIME INDEX J
85*      DO 106 J=1,MXT
86*      C      M AND N TAKE UP VALUES 1,2 AND 3 CALCULATED FROM J
87*      M = MOD(J,3) + 1
88*      N = MOD(J-1,3)+1
89*      C      DO LOOPS FOR SECTIONS OF ROD
90*      C      DIFFUSION COEFFICIENTS CHANGE WITH J AND I BUT NOT WITH K
91*      DO 108 I=1,NLM
92*      IF(I.EQ. 1) GO TO 114
93*      IF(THSOF(I,N).NE. 0.0) GO TO 132
94*      THSOF(I,N) = 0.0
95*      PROX(I,N) = THK
96*      GO TO 110
97*      132 D(I,M) = DO*EXP(-E/2./T(I,N))
98*      KN = 0
99*      DDT(I,M) = DT/FT
100*      134 KN = KN+1
101*      DDT(I,M) = DDT(I,M)/KN
102*      TAM = D(I,M)*DDT(I,M)/PROX(I,N)
103*      IF(TAM.GT. 0.5*THSOF(I,N)) GO TO 134
104*      THSOF(I,M) = THSOF(I,N)
105*      PROX(I,M) = PROX(I,N)
106*      IFT(I,M) = IFIX(DT/DDT(I,M))
107*      KFT = IFT(I,N)
108*      C      MATERIAL DIFFUSION DURING EACH DT
109*      DO 124 L=2,KFT
110*      TAM = D(I,M)*DDT(I,M)/PROX(I,M)
111*      IF(TAM.GT. THSOF(I,M)) TAM=THSOF(I,M)
112*      THSOF(I,M) = THSOF(I,M)-TAM
113*      PROX(I,M) = PROX(I,M)+TAM*(1. + HOVS)
114*      IF(THSOF(I,M).GT. 1.0E-08*XSOF) GO TO 124
115*      THSOF(I,M) = 0.0
116*      PROX(I,M) = THK
117*      GO TO 110

```

```

118*      124 CONTINUE
119*  C      CALCULATE F(I,M) AND CHANGE IN F(I,M)
120*  110 F(I,M) = THSOE(I,M)/XSOF
121*      DELE = F(I,M)*F(I,M)
122*      IF(DELE .GT. 0.0) DELE = 0.0
123*  C      CALCULATE HEAT EVOLUTION (CAL/CM**3)
124*      HEV = -RO*G*DELE
125*  C      CALCULATE HEAT RADIATION (CAL/CM**3)
126*      DELH = HEV
127*  C      CALCULATE HEAT CONDUCTION INDEPENDENTLY OF RADIATION AND REACTION
128*      IF(J .GE. 2) GO TO 116
129*      114 T(I,M) = P*(T(I,N)+FACT1*T(I+1,N))-(P*FACT2-1.)*T(I,N)
130*      TAM = (Y(I,M)*ACU+T(I,N)*AIN)/X1**2
131*      T(I,M) = TAM
132*      GO TO 108
133*      116 T(I,M) = P*(T(I-1,N)+FACT1*T(I+1,N))-(P*FACT2-1.)*T(I,N)
134*  C      READJUST TEMPERATURE FOR RADIATION AND REACTION
135*      T(I,M) = T(I,M) + DELH/C/RO
136*      108 CONTINUE
137*  C      BOUNDARY CONDITIONS
138*      T(NL,M) = T(UL-2,M)
139*      IF(J .LE. 100 .AND. MOD(J,10) .EQ. 0) GO TO 126
140*      IF(J .LE. 50 .AND. MOD(J,5) .EQ. 0) GO TO 126
141*      IF(J .LE. 10 .AND. MOD(J,2) .EQ. 0) GO TO 126
142*      IF(J .EQ. 1) GO TO 126
143*  C      FOR PRINTOUT PATTERN
144*      IF(J .LE. 500 .AND. MOD(J,50) .EQ. 0) GO TO 126
145*      IF(J .GT. 500 .AND. MOD(J,100) .EQ. 0) GO TO 126
146*      GO TO 106
147*  C      HEADING FOR PRINTOUT OF ARRAYS
148*      126 WRITE(6,406)
149*      DO 128 I=1,NLM
150*          TIME = J*DT
151*          DIST = (FLOAT(I) - 1.5)*DX
152*          WRITE(6,408) J, TIME, I, DIST, F(I,M), T(I,M), D(I,M), DDT(I,M),
153*          *THSOE(I,M), PROX(I,M)
154*      128 CONTINUE
155*      DO 142 I=2,NLM
156*          II = I-1
157*          IF(II .NE. 1 .AND. MOD(II,10) .NE. 0) GO TO 142
158*          LSOF = IFIX(THSOE(I,M)/XPERS)
159*          IF(THSOE(I,M)/XPERS = FLOAT(LSOF) .GT. 0.5) LSOF = LSOF+1
160*          IF(LSOF .LE. 0) LSOF=1
161*          LPROX = IFIX(PROX(I,M)/XPERS)
162*          IF(PROX(I,M)/XPERS = FLOAT(LPROX) .GT. 0.5) LPROX = LPROX+1
163*          IF(LPROX .LE. 0) LPROX=1
164*          LHAR = 110 - LSOF - LPROX
165*          IF(LHAR .LE. 0) LHAR=1
166*          ENCODE(PRINT7,430) LSOF
167*          V(7) = PRINT7
168*          ENCODE(PRINT9,430) LPROX
169*          V(9) = PRINT9
170*          ENCODE(PRINT11,430) LHAR
171*          V(11) = PRINT11
172*          WRITE(6,V) II
173*      142 CONTINUE
174*      106 CONTINUE
175*      END

```


APPENDIX IV

METHOD FOR COMPUTING IGNITION CHARACTERISTICS

The method for computing the ignition characteristics from a computer run is illustrated for a Ti-C mixture. The computer output has been plotted on Figure 8. Table IV-1 lists the temperatures at the center of the first slice of a rod-shaped reaction mixture for various time increments until the temperature of the first slice equals the igniter temperature of 800°K. At this time, the heat flux into the first slice vanishes, and the total increase of sensible heat in the slice is the ignition energy, and the average of the temperature gradients multiplied by the thermal conductance becomes the average ignition flux.

TABLE IV-1 METHOD OF IGNITION FLUX CALCULATION

Input Parameters

Thermal Conductivity: 0.017 cal/cm-sec-°K
 Heat Capacity at 800°K: 0.20 cal/g-°K
 Half Thickness of Slice, $1/2 \Delta x = 0.004$ cm
 Temperature of Source: 800°K
 Contact Time with Source: Continuous
 Unit Time Increment, $\Delta t = 0.1742$ msec

Slice Temp. T (°K)	Temp. Diff. ΔT (°K)	Time (msec)	Temp. Gradient $\Delta T / 1/2 \Delta x$ (°K/cm $\times 10^4$)	Ignition Flux (cal/cm ² sec)	Change of Temp. With Time ($\Delta T / \Delta t \times 10^6$)
300	500	0	12.4	2120	2.86
341.7	458.3	0.1742	11.5	1952	2.63
376.4	423.6	0.3484	10.6	1800	2.43
430.6	369.4	0.6968	9.24	1570	2.12
470.9	329.1	1.0452	8.24	1400	1.89
527.5	272.5	1.742	6.80	1156	1.56
607.6	192.4	3.484	4.80	816	1.10
654.0	146.0	5.226	3.64	620	0.838
686.3	113.7	6.968	2.82	480	0.650
732.0	68.0	10.452	1.70	290	0.390
800	0	14.5	0	0	0

Results

Ignition Time * 14.5 msec
 Average Ignition Flux over 14.5 msec 470 cal/cm² sec
 Ignition Energy ** 2260 cal/g

*Ignition time is less than ignition delay, as ignition delay is the time required to approach reaction temperature.

**Energy: $C_p \sum \frac{\Delta T}{\Delta t} t$

REFERENCES

1. R. Hultgren, R. L. Orr, P. D. Anderson, and K. K. Kelley, *Selected Values of Thermodynamic Properties of Metals and Alloys*, John Wiley & Sons, N.Y., 1963
2. R. Hultgren, R. L. Orr and K. K. Kelley, "Supplement to Selected Values of Thermodynamic Properties of Metals and Alloys," Department of Metallurgy, University of California, Berkeley.
3. Pyrofuze Engineering Datalog, Pyrofuze Corporation, Mount Vernon, New York
4. P. N. Laufman, *Space/Aeronautics*, 152, April 1970
5. L. G. Fasolino, "Thermodynamic Properties of Bi-Metallic Powders," Quarterly Letter Report, Nonr-3608 (00), Project No. 44-1-0026, National Research Corporation, 9 November 1962
6. C. E. Wicks and F. E. Block, "Thermodynamic Properties of 65 Elements Their Oxides, Halides, Carbides and Nitrides," U. S. Bureau of Mines Bulletin 605, 1963
7. A. P. Bayanov, *Zh. Fiz. Khim.*, 43 (9), 2231-3, 1969
8. M. I. Ivanov, V. A. Tumbakov, *Atomnaya Energia, SSSR*, 7, (1) 33-6 (1969)
9. D. B. Novotny and J. F. Smith, U.S. Atomic Energy Commission IS 589 (1963)
10. P. M. Arzhanyi, R. M. Volkova, D. A. Prokoshkin, *Dokl. Akad. Nauk SSSR* 150 (1), 96-8 (1963)
11. M. P. Morozova, G. A. Rybakova, *Vestn Leningrad Univ. Fiz. Khim.*, 23, (22) 171-3 (1968)
12. S. Aronson and A. Auskern, U. S. Atomic Energy Commission BNL-9167 (1965)

13. G. V. Samsonov: No. 2 Properties Index, Plenum Press Handbooks of High Temperature Materials, Plenum Press, N.Y., 1964
14. F. S. Domalski and G. T. Armstrong, J. Res. Nat. Bur. Std. A 72, (2) 133-9 (1968)
15. W. A. Knarr, Diss. Abstr. 20, 4541 (1960)
16. K. E. Spear II, U.S. Atom. Energ. Comm. 1967, C001140-157
17. G. K. Johnson, E. Greenberg, J. L. Margrave, J. Chem. Eng. Data 12, (4) 597-600 (1967)
18. O. Kubaschewski and G. Heymer, Trans. Farad. Soc., 56, 473-8, (1960)
19. D. D. Wagman et al., "Selected Values of Chem. Therm. Prop.," NBS Tech. Notes 270-3, 270-4, 1968
20. A. Schneider, H. Klotz, J. Stendel, G. Strauss, Pure Appl. Chem. 2, 13-15 (1961)
21. G. R. Cunningham, F. J. Smith and W. Bradshaw, AIAA Paper 65-644 AIAA Thermophysics Specialists Conference, Monterey, California, Sep 1965
22. G. D. Sturgeon and H. A. Eick, J. Phys. Chem., 69, (11)
23. P. Chiotti, J. A. Kateley, J. Nucl. Mater., 32 (1), 135-45 (1969)
24. V. V. Akachinski, L. M. Koltin, M. I. Ivanov and N. S. Podolskaya, Proc. Symp. Thermodyn. of Nuclear Materials, Vienna 1962, Paper 309-17
25. R. H. Flowers and E. G. Rauh, U. K. Tom. Energ. Auth. Res. Group, Atom. Energ. Res. Establ. Rept. AERE-R 5011 (1965)
26. A. D. Mah, U.S. Bur. Mines Rept. Invest. 6415 (4) 1964
27. D. E. Jackson, R. G. Bedford, G. W. Barton, U.S. Atom. Energ. Comm., UCRL 7362 T (1963)
28. E. A. Dancy, L. H. Evertt, C. L. McCabe, Trans. Met. Soc. AIME 224, 1095-1104 (1962)

29. H. K. Lonsdale, J. N. Graves, *Thermodyn. Nucl. Matr., Proc., Symp.*, Vienna, 601-23 (1963)
30. J. C. d'Entremont, J. Chipman, *J. Phys. Chem.*, 67, 499-501 (1963)
31. K. Grjotheim, O. Herstad, S. Petrucci, R. Skarbo, J. Toquiri, *Rev. Chim., Acad. Rep. Populaire Roumaine* 7, (1) 217-23 (1962)
32. T. Gross, C. Hayman, H. Clayton, *Thermodyn. Nucl. Mat., Proc. Symp.*, Vienna, 601-23 (1963)
33. P. V. Gel'd, S. M. Letun, N. N. Serebrennikov, *Izv. Vyssh. Ucheb. Zaved., Chern. Met.*, 9, (12) 5-13 (1966)
34. G. F. Voronium, Nguyen Thanh Hien, *Zhur. Fiz. Khim.*, 41, (6) 1468-70 (1967)
35. V. N. Eremenko and G. M. Lukashenko, *izv. Akad. Nauk SSSR, Neorg. Matr.* 1, (8) 1296-7 (1965)
36. V. N. Eremenko and G. M. Lukashenko, *Ukr. Khim. Zhur.*, 29, (9), 896-900 (1963)
37. I. Johnson, M. Chasanov, R. Yonco, *Trans. Met. Soc. AIME* 233, (7), 1408-14 (65)
38. G. J. Gartner and P. Chiotti, *Metals, Ceramics and Materials (UC-25)*, TID-4500, 1 Dec 1964, U.S. Atom. Energ. Comm IS 1070
39. A. V. Volkovich, I. F. Nichkov, *Zhur. Fiz. Khim.*, 42, (3) 682-5 (1968)
40. J. R. Guadagno, R. L. Orr, R. Hultgren, *U.S. Army Contract DA-04-200-ORD-171*, Sep 1, 1961
41. J. H. Carpenter and A. W. Searey, *J. Phys. Chem.*, 67, (10) 2144-7 (1963)
42. H. S. Carslaw and J. C. Jaeger, *"Conduction of Heat in Solids,"* Oxford, 1959
43. J. H. Westbrook, Editor, *Intermetallic Compounds*, John Wiley & Sons, Inc. Chapter 20, New York, 1967
44. G. V. Samsonov and A. P. Epik, "Investigation of Conditions of Surface Saturation of Refractory Transition Metals by Carbon and Boron," *Akad. Nauk USSR*, p. 132-139, reprint courtesy of author, no vol., no date

45. "20 mm CERMET Projectile," RFP F08651-71-R-0632, "CERMET Munitions," RFQ F08635-71-Q-0177
46. Eglin Air Force Base, Florida, Development of an Experimental Inter-metallic-Forming Starter System for the M1 Smoke (HC) Canister by R. L. McKenney, Jr. AFATL-TR-71-136, October 1971.
47. R. V. Rosman, D. B. Oliver, and J. H. Huntington, Effects of Radiation on Propellant Systems (U), Aug 1970, AFRPL-TR-70-109, Contract No. F04611-C-0062
48. B. W. Travor, Qualification of Close Tolerance Time Delays Employing Pyrofuze Wire, Frankford Arsenal, Mar 1970, ASD-TR-70-13, FAR, 1949
49. H. H. Helms, Jr., A. G. Rozner, "Pyronol and Associated Pyrotechnic Devices," 2 Jun 1970, Magnetism and Metallurgy Division (211), Naval Ordnance Laboratory, Silver Spring, Maryland
50. A. P. Hardt, "Study of Tracer Munitions Using Intermetallic Reactions," LMSC-D081722, 15 Mar 1971, Technical Proposal to Frankford Arsenal
51. N. E. Weare, "Exothermic Brazing of Metallic Parts," U.S. Patent 3,358,356, 1967; also, R. A. Long, "Exothermic Brazing of Refractory Metals," Met. Soc. Conf., 30, pp. 249-258, 1966
52. H. Caveny, "Bimetallic Fibers in Solid Propellants," U.S. Patent 3,508,494

UNCLASSIFIED

Security Classification

DOCUMENT CONTROL DATA - R & D		
(Security classification of title, body of abstract and indexing annotation must be entered when the overall report is classified)		
1. ORIGINATING ACTIVITY (Corporate author) Lockheed Palo Alto Research Laboratory Lockheed Missiles & Space Company Palo Alto, California 94304		2a. REPORT SECURITY CLASSIFICATION UNCLASSIFIED
3. REPORT TITLE INCENDIARY POTENTIAL OF EXOTHERMIC INTERMETALLIC REACTIONS		2b. GROUP
4. DESCRIPTIVE NOTES (Type of report and inclusive dates) Final Report - 19 March 1970 to 19 May 1971		
5. AUTHOR(S) (First name, middle initial, last name) Alexander P. Hardt		
6. REPORT DATE July 1971	7a. TOTAL NO. OF PAGES 76	7b. NO. OF REFS 52
8a. CONTRACT OR GRANT NO. F08635-70-C-0063	9a. ORIGINATOR'S REPORT NUMBER(S) LMSC-D177523	
b. PROJECT NO. 1082	9b. OTHER REPORT NO(S) (Any other numbers that may be assigned this report)	
c. Task No 01	AFATL-TR-71-87	
d. Work Unit 002		
10. DISTRIBUTION STATEMENT Distribution limited to U. S. Government agencies only; other agencies and personnel <i>Test and Evaluation</i> other agencies and personnel , distribution limitation applied July 1971. Other requests for this document must be referred to the Air Force Armament Laboratory (DLIF), Eglin Air Force Base, Florida 32542-		
11. SUPPLEMENTARY NOTES Available in DDC		12. SPONSORING MILITARY ACTIVITY Air Force Armament Laboratory Air Force Systems Command Eglin Air Force Base, Florida 32542
13. ABSTRACT The objective of this research was to study the incendiary potential of intermetallic reactions. A thorough literature review of the thermochemistry of exothermic alloy formation, measurement of the reaction rates, reaction temperatures, and ignition characteristics of loose and pressed binary and tertiary mixed powders provided basic information for incendiary assessment. The borides, carbides, and aluminides of titanium, zirconium, and nickel were found to offer the greatest promise. The data were compared with those obtained by a computerized heat transfer analysis of rod shaped and hollow cylindrical geometries. The rate controlling parameters were found to be particle size, thermal conductivity, heat of reaction, and diffusivity. In most cases it was found that reaction characteristics were independent of particle size distribution, particle shapes, contamination, bulk density, and compaction. Experimental data agreed with analytical predictions. Intermetallic reactions were deemed to be a novel class of reactions and the results were found to have wide applicability in improving the performance characteristics of pyrotechnic, ordnance, and incendiary devices.		

DD FORM 1 NOV 65 1473

UNCLASSIFIED

Security Classification

UNCLASSIFIED

Security Classification

14. KEY WORDS	LINK A		LINK B		LINK C	
	ROLE	WT	ROLE	WT	ROLE	WT
Incendiary Pyrotechnic Igniter Ignition Energy Ignition Delay Delay Fuzes Intermetallic reaction Thermite reaction						

UNCLASSIFIED

Security Classification